DISSERTATIONES
GEOPHYSICALES
UNIVERSITATIS
TARTUENSIS
32

JORMA RAHU

Novel insights into aerosol-cloud interactions by analysing the temporal evolution of strong anthropogenic cloud perturbations

DISSERTATIONES GEOPHYSICALES UNIVERSITATIS TARTUENSIS
32

DISSERTATIONES GEOPHYSICALES UNIVERSITATIS TARTUENSIS
32

JORMA RAHU

Novel insights into aerosol-cloud interactions by analysing the temporal evolution of strong anthropogenic cloud perturbations

UNIVERSITY OF TARTU
Press
1632

This study was carried out at the University of Tartu, Institute of Physics, Centre for Climate Research.

The Dissertation was admitted on April 9th, 2025, in partial fulfilment of the requirements for the degree of Doctor of Philosophy in Physics and allowed for defence by the Council of the Institute of Physics, University of Tartu.

Supervisors: Velle Toll, PhD, Associate Professor in Climate Physics, Centre for Climate Research, Institute of Physics, University of Tartu, Estonia

Piia Post, PhD, Professor of Climate Science, Centre for Climate Research, Institute of Physics, University of Tartu, Estonia

Opponent: Harri Kokkola, Research Professor, Finnish Meteorological Institute, Finland

Defence: June 12th, 2025

ISSN 1406-0310 (print)
ISBN 978-9916-27-884-0 (print)
ISSN 2806-2329 (pdf)
ISBN 978-9916-27-885-7 (pdf)

University of Tartu Press
www.tyk.ee

CONTENTS

LIST OF ORIGINAL PUBLICATIONS

This thesis is based on the following original publications, which are referred to by their Roman numerals in the text.

I **Rahu, J.**, Trofimov, H., Post, P., Toll, V. (2022). Diurnal evolution of cloud water responses to aerosols. *Journal of Geophysical Research: Atmospheres*, *127*, e2021JD035091. https://doi.org/10.1029/2021JD035091

II Toll, V., **Rahu, J.** (2023). Strong anthropogenic cloud perturbations can persist for multiple days. *Journal of Geophysical Research: Atmospheres*, *128*, e2022JD038146. https://doi.org/10.1029/2022JD038146

III Toll, V., **Rahu, J.**, Keernik, H., Trofimov, H., Voormansik, T., Manshausen, P., Hung, E., Michelson, D., Christensen, M. W., Post, P., Junninen, H., Murray, B. J., Lohmann, U., Watson-Parris, D., Stier, P., Donaldson, N., Storelvmo, T., Kulmala, M., Bellouin, N. (2024). Glaciation of liquid clouds, snowfall, and reduced cloud cover at industrial aerosol hot spots. *Science,* 386, 756–762. https://doi.org/10.1126/science.adl0303

Author's contributions

I Formal analysis, figures, contributed to study design, and wrote the original manuscript.

II Formal analysis, figures, contributed to study design, contributed to writing the manuscript.

III Formal analysis, figures, contributed to writing the manuscript.

ABSTRACT

The Earth's climate is governed by radiative energy fluxes entering and leaving the climate system. Aerosol particles act as cloud condensation nuclei and ice-nucleating particles, strongly affecting cloud properties. How clouds respond to anthropogenic aerosols is the most uncertain component of the anthropogenic forcing of Earth's climate. Here, I use geostationary satellite observations and ground-based precipitation radar data to study the temporal evolution of aerosol-polluted clouds to improve the physical understanding of aerosol impacts on clouds. In some cases, there is a substantial increase in the amount of liquid cloud water in the afternoon in polluted clouds compared to unpolluted clouds. However, most often, polluted clouds are thinner than nearby unpolluted clouds. Using geostationary satellite data, I show that polluted cloud tracks polluted by aerosols from isolated industrial sources are relatively long-lived, with a median lifetime of 18 hours. There are multiple cases where polluted cloud tracks are visible for multiple consecutive days, 84 hours in the most extreme case. Such long lifetimes indicate that, at least in some cases, polluted cloud tracks could fully adjust to aerosol-induced increases in cloud droplet numbers, reaching the quasi-equilibrium state. Furthermore, I found evidence for decreases in cloud cover in response to anthropogenic aerosols acting as ice-nucleating particles. Anthropogenic ice-nucleating particles lead to the glaciation of supercooled liquid water clouds, as detected in satellite observations, and snowfall, as detected in ground-based precipitation radar observations. It is important to note that the emission of heat and water vapour may also play a role in the observed glaciation events. Analysis of the temporal evolution of strong anthropogenic cloud perturbations led to the improved process-level understanding of aerosol-cloud interactions presented in this work and could ultimately lead to more reliable climate projections.

ABBREVIATIONS

List of acronyms

ABI	Advanced Baseline Imager
CCN	Cloud condensation nuclei
CDS	Climate Data Store
CPP	Cloud Physical Properties
CTT	Cloud top temperature
DAC	Data Access Client
ECMWF ERA5	European Centre for Medium-Range Weather Forecasts Re-analysis v5
ESDIS	Earth Science Data and Information System
EUMETSAT	European Organisation for the Exploitation of Meteorological Satellites
FCI	Flexible Combined Imager
GIBS	Global Imagery Browse Services
GOES-R	Geostationary Operational Environmental Satellites R Series
INP	Ice-nucleating particle
IPCC	Intergovernmental Panel on Climate Change
KNMI	The Royal Netherlands Meteorological Institute
MODIS	Terra Moderate Resolution Imaging Spectroradiometer
MSG SEVIRI	Meteosat Second Generation Spinning Enhanced Visible Infra-Red Imager
MTG	Meteosat Third Generation
NASA	National Aeronautics and Space Administration
RGB	Red-Green-Blue
US	United States
UTC	Coordinated Universal Time

List of variables

COD	Cloud optical depth
LWP	Liquid water path $\left[\frac{g}{m^2}\right]$
R_{eff}	Cloud droplet effective radius $[\mu m]$
S	Snowfall rate $\left[\frac{mm}{h}\right]$
Z	Radar reflectivity factor $\left[\frac{mm^6}{m^3}\right]$

1. INTRODUCTION

1.1 Aerosol impacts on clouds and Earth's climate

Climate change since the industrial revolution is a tug-of-war between anthropogenic greenhouse gas warming and aerosol cooling (IPCC, 2023). Tiny solid and liquid air pollution particles, aerosols, suspended in the atmosphere, exert a considerable influence on Earth's climate both directly and indirectly (Bellouin et al., 2020). Directly through interacting with solar and terrestrial radiation, indirectly through modulating cloud properties. The net effect of aerosols on Earth's climate is cooling, offsetting part of the greenhouse gas warming effect (Bellouin et al., 2020; IPCC, 2023). However, the magnitude of the aerosol cooling effect on Earth's climate is highly uncertain, hindering accurate future climate projections (Bellouin et al., 2020). As aerosol cooling is the most uncertain component of anthropogenic climate forcing, reduced uncertainty in aerosol forcing could substantially decrease overall uncertainty in anthropogenic climate forcing (Bellouin et al., 2020; Watson-Parris and Smith, 2022; IPCC, 2023).

Aerosol particles affect cloud properties and, therefore, global radiative fluxes through a variety of physical mechanisms. The Twomey effect (Twomey, 1974; Quaas et al., 2020) refers to the effect of how increased aerosol concentrations can increase cloud droplet numbers and cloud albedo. In essence, when more aerosol particles are present in the atmosphere, they serve as additional CCN, resulting in a larger number of smaller cloud droplets when the total LWP remains constant. This results in clouds with higher albedo, as the increased number of smaller droplets means a higher total surface area of droplets to scatter incoming solar radiation. On the other hand, smaller cloud droplets have reduced collision and coalescence efficiency, which means they are less likely to merge and form larger cloud droplets. This suppresses the precipitation formation, as the droplets struggle to grow large enough to fall as rain. Consequently, such clouds can have increased thickness and coverage, and they tend to remain longer in the atmosphere (Albrecht, 1989; Suzuki et al., 2013). From the other side, a higher number of smaller cloud droplets could evaporate more efficiently and lead to aerosol-enhanced entrainment, i.e. enhanced mixing of the cloud layer with the drier ambient air (Ackermann et al., 2004; Bretherton et al., 2007; Small et al., 2009). The aerosol-enhanced entrainment can ultimately reduce cloud thickness, lifetime and vertical development (Small et al., 2009). It has been suggested that the net effect is determined by whether the clouds are precipitating or not (Toll et al., 2019; Bellouin et al., 2020; IPCC, 2023).

At temperatures below 0 °C, anthropogenic aerosols can also serve as INPs and transform supercooled liquid-water cloud droplets into ice crystals (Cziczo et al., 2009; Zhao et al., 2019). Importantly, at a given temperature and atmospheric pressure, the saturation water vapour pressure over ice is lower than over liquid water droplets. This difference causes water vapour to preferentially deposit onto ice crystals, causing them to grow larger at the expense of liquid-phase cloud droplets (Wegener, 1911; Bergeron, 1935; Findeisen, 1938). As a result,

ice crystals quickly become dominant in mixed-phase clouds, leading to potential formation of snowfall. This process is commonly known as the Wegener-Bergeron-Findeisen process (Storelvmo and Tan, 2015; Wegener, 1911; Bergeron, 1935; Findeisen, 1938).

The magnitude of the impacts of anthropogenic aerosols serving as CCN on clouds and radiation fluxes is highly uncertain (IPCC, 2023; Bellouin et al., 2020). Moreover, while the Twomey effect is physically well understood, the cloud thickness and cloud fraction adjustments due to suppression of precipitation and aerosol-enhanced entrainment caused by increased cloud droplet numbers remain poorly understood. In addition, due to the lack of laboratory evidence that anthropogenic aerosol particles can act as INPs, their impacts on supercooled cloud droplets have been excluded from the climate-forcing estimates in the latest IPCC Assessment Report (IPCC, 2023).

The uncertainty in climate forcing by aerosol impacts on clouds can be partially attributed to the poor process-level understanding of aerosol-cloud interactions at both microphysical and macrophysical levels (Bellouin et al., 2020). In addition, the ambient meteorological conditions affect both clouds and aerosols, which is referred to as meteorological covariability (Gryspeerdt et al., 2016; Goren et al., 2024; Mauger and Norris, 2007). Owing to the meteorological covariability, it is difficult to unravel the causal influence of aerosols on clouds (Gryspeerdt et al., 2016; Goren et al., 2024). Recent studies using natural experiments of aerosol-cloud interactions, like ship-track-like aerosol-polluted cloud tracks, have given new insights to better bound the climate forcing by aerosol-cloud interactions (Manshausen et al., 2022; Toll et al., 2019; Yuan et al., 2023). In the case of ship-track-like aerosol-polluted cloud tracks, only the level of aerosol pollution changes between the polluted and nearby unpolluted areas, while the meteorological conditions are similar for both regions (Christensen et al., 2022; Toll et al., 2019). This means it is possible to use aerosol-polluted cloud tracks as natural experiments, where experiment-like conditions occur without any intervention by the researcher (Christensen et al., 2022).

In this thesis, I have used ship-track-like industry-polluted cloud tracks as natural experiments, similarly to previous research by Toll et al. (2019), Trofimov et al. (2020), and Trofimov et al. (2022). Strong ship-track-like industrial cloud perturbations have been previously found in stratocumulus (stratiform) cloud decks (Toll et al., 2019). An important novelty of my work compared to previous work on industry tracks is the analysis of the temporal evolution of the cloud responses to aerosols within the aerosol-polluted cloud tracks. High spatial resolution polar orbit satellite data has given valuable insights into aerosol-cloud interactions but, unfortunately, lacks temporal resolution. On the other hand, there are high temporal resolution geostationary data with comparatively lower spatial resolution. The temporal evolution of ship tracks has been previously studied at the dense marine traffic corridor on the west coast of Africa, which is a highly favourable location for the use of MSG SEVIRI satellite data (Schreier et al., 2010). When viewed from satellite imagery, ship tracks have relatively high contrast due to the dark and pristine oceanic background conditions. This is often

not the case for continental industry tracks. As industry tracks are usually wider compared to ship tracks (Trofimov et al., 2020), the industry tracks can also be seen from geostationary satellite data with relative ease. My work, as far as I am aware, is the first to study industry tracks using geostationary satellite data.

While the cloud droplet numbers can increase just within minutes in response to additional aerosols (Gryspeerdt et al., 2021), other cloud responses develop over longer timescales while the cloud adjusts to the increased droplet numbers. Using Large-Eddy-Simulation models, it has been shown that for non-precipitating stratocumulus clouds, these adjustments can take up to 20 hours until reaching the new equilibrium state (Glassmeier et al., 2021), emphasising the importance of understanding the temporal evolution of cloud responses to aerosols. Furthermore, accounting for the temporal evolution of cloud responses to aerosols is critical for the reliable quantification of aerosol impacts on clouds based on satellite remote sensing data (Gryspeerdt et al., 2021).

1.2 Research Goals

The main aim of this thesis was to improve the physical understanding of aerosol impacts on clouds by analysing the temporal evolution of strong anthropogenic aerosol perturbations on clouds. Polluted cloud tracks provide striking visual evidence that increased aerosol loading changes cloud properties. Moreover, aerosol-polluted cloud tracks can be used to better understand aerosol impacts on clouds and Earth's climate, although the representativeness of track responses to climatological cloud responses to anthropogenic aerosols is still uncertain (Toll et al., 2019; Christensen et al., 2022). Therefore, research on aerosol-polluted cloud tracks should try to assess the representativeness of aerosol-polluted cloud tracks for quantifying anthropogenic aerosol forcing. Significant uncertainty comes from the temporal evolution of pollution tracks. Using geostationary satellite data and ground-based precipitation radar data, I provide unique insights into the temporal evolution of aerosol-polluted cloud tracks that are impossible to observe using satellite data from polar orbiters.

List of specific research goals:

1. To identify aerosol-polluted cloud tracks from geostationary satellite data [I–III].
2. To quantify the diurnal evolution of cloud responses to anthropogenic aerosols [I].
3. To quantify the lifetime of aerosol-polluted cloud tracks based on the visibility of tracks in geostationary satellite data [II].
4. To develop a physical understanding of anthropogenic glaciation of supercooled liquid-water clouds [III].
5. To quantify the duration and intensity of glaciation-induced snowfall using ground-based precipitation radar data [III].

1.3 Theses

1. Continental anthropogenic pollution tracks in clouds are reliably detectable from geostationary satellite data, which allows to study fast-evolving temporal evolution of cloud responses to aerosols [I–III].
2. Under certain meteorological conditions, polluted clouds gradually grow thicker in the afternoon [I].
3. Strong continental anthropogenic cloud perturbations are long-lived, many remaining visible for multiple days [II].
4. The lifetime of continental pollution tracks is heavily influenced by the local cloud regime and ambient meteorological conditions [II].
5. Anthropogenic aerosols act as ice-nucleating particles at different anthropogenic aerosol sources like factories processing metals and minerals [III].
6. Observing the temporal evolution of anthropogenic glaciation of supercooled liquid-water clouds using geostationary satellite data and ground-based precipitation radar data reveals the causal sequence from glaciation to snowfall to reduced cloud cover [III].

2. METHODS

2.1 General study design for the analysis of the temporal evolution of anthropogenic cloud perturbations

Anthropogenic aerosol particles from various air pollution sources can strongly affect the physical characteristics of clouds. Both visible (Toll et al., 2019) and invisible (Manshausen et al., 2022) aerosol-polluted cloud tracks have been previously detected, as anthropogenic aerosols serving as CCN redistribute liquid cloud water among a larger number of smaller cloud droplets (Twomey, 1974). A rare subset of anthropogenic aerosols can also act as INPs, glaciating supercooled liquid cloud droplets, decreasing cloud fraction and creating ice clouds with lower albedo than surrounding unpolluted liquid clouds ([III]; Chen et al., 2024; Zhao et al., 2019). Visual cloud disturbances induced by anthropogenic aerosols can be easily identified in satellite data by relying on the characteristic signature of enhanced near-infrared reflectance in CCN-polluted clouds (Toll et al., 2019; Coakley et al., 1987) or decreased cloud fraction in the case of INPs [III].

Therefore, for all of the studies [I]–[III], I identified most of the pollution track cases initially using satellite images from the US NASA GIBS through the Worldview application. NASA GIBS is part of the NASA ESDIS. I mostly used the Terra MODIS Corrected Reflectance RGB composites (Platnick, 2015; Salomonson, 1989) that rely on the measurements in Bands 3, 6 and 7 (corresponding bandwidths are 459–479 nm, 1628–1652 nm, 2105–2155 nm). Due to the relatively high spatial resolution of MODIS data (250 m for bands 1–2, 500 m for bands 3–7), the polluted cloud tracks, most often having a width of 10 kilometres or more, can be detected in the satellite images by the naked eye (Figure 1). Terra MODIS temporal resolution is roughly one image per 24 h for the same location on the Earth.

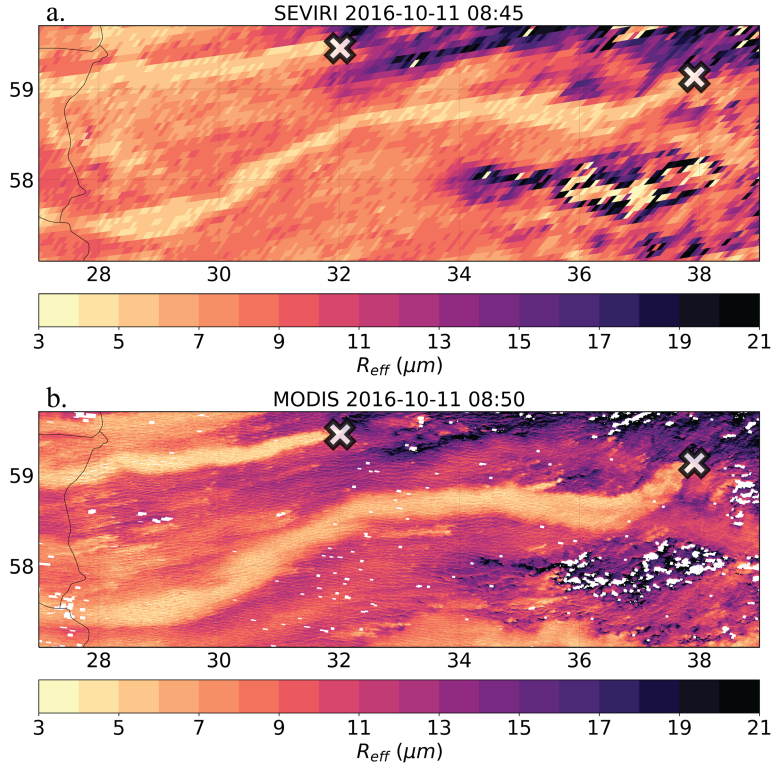

Figure 1. Aerosol-polluted industrial cloud tracks originating from metallurgical sites in Russia [I]. Colours depict cloud droplet effective radius, where yellowish areas show clouds with reduced droplet sizes due to added aerosols. (a) Spinning Enhanced Visible and Infrared Imager (SEVIRI), and (b) Moderate Resolution Imaging Spectroradiometer (MODIS) data.

Fast-evolving changes in cloud properties were analysed with geostationary satellite data. Over Europe, the MSG SEVIRI data were used (Aminou, 2002). SEVIRI raw data serves as input for the CPP product (Roebeling et al., 2006; MSG-CPP, 2012), which was used to study both the micro- and macrophysical properties of aerosol-polluted and surrounding unpolluted clouds with 15-minute temporal resolution. 5-minute temporal resolution GOES-R ABI (Schmit et al., 2017; Schmit and Gunshor, 2020) data were used over the Americas (including Canada). For more accurate cloud top temperature comparisons, the MODIS CTT product (Platnick et al., 2015) was also used.

2.2 Analysis of the diurnal evolution of cloud responses to aerosols

In study [I], I used geostationary MSG SEVIRI satellite data to study the diurnal evolution of strong anthropogenic cloud perturbations [I]. The focus was on continental heavy industrial sites in the European part of Russia, such as steel production factories, chemical industries, oil refineries, and large mines (Table 1). For the study area, the spatial resolution of the SEVIRI satellite data was around 10 km per pixel, on average. In total, I identified 23 track days from 2006 to 2017, where aerosol-polluted cloud tracks were seen downwind of the studied air pollution sources (Table 1) in the study region. More cloud condensation nuclei lead to increased cloud droplet number concentrations and smaller cloud droplets. Smaller cloud droplets mean that polluted cloud areas stand out from the nearby unpolluted clouds in the near-infrared spectrum (e.g. Toll et al., 2019).

Table 1. List of aerosol emission sources (at city scale) sampled in study [I]. This table is adapted from [I].

City	(Latitude, Longitude)	Type of industry
Cherepovets	(59.13, 37.92)	metallurgy and chemical industry
Yaroslavl	(57.62, 39.85)	machine factory
Chagoda	(59.17, 35.33)	glass factory
Ryazan	(54.60, 39.70)	electronics factory and oil refinery
Kirishi	(59.45, 32.02)	oil refinery and chemical industry
Novomoskovsk	(54.08, 38.22)	chemical industry
Moscow	(55.75, 37.62)	chemical, textile and car-building industry
Veliky Novgorod	(58.52, 31.28)	chemical and radio-electronic industry
Lipetsk	(52.62, 39.60)	metallurgy, machinery, chemical industry
Stary Oskol	(51.30, 37.83)	iron ore mine
Nizhny Novgorod	(56.33, 44.01)	auto industry, ship, and aircraft factories
Saratov	(51.53, 46.02)	oil refinery, aerospace manufacturing industry

The initial identification of the pollution track cases relied on the near-infrared signatures. The next step was to perform the semi-automatic classification of cloud properties as polluted and unpolluted (Figure 2), based on cloud droplet effective radius retrieved from geostationary MSG SEVIRI satellite data provided within the CPP product. Although SEVIRI has infrared channels allowing for observations during both day and nighttime, the CPP product, similarly to other retrievals of cloud properties based on passive satellite remote sensing, relies on backscattered solar radiation, which means the use is limited to daytime analysis only (Benas et al., 2023; Roebeling et al., 2006).

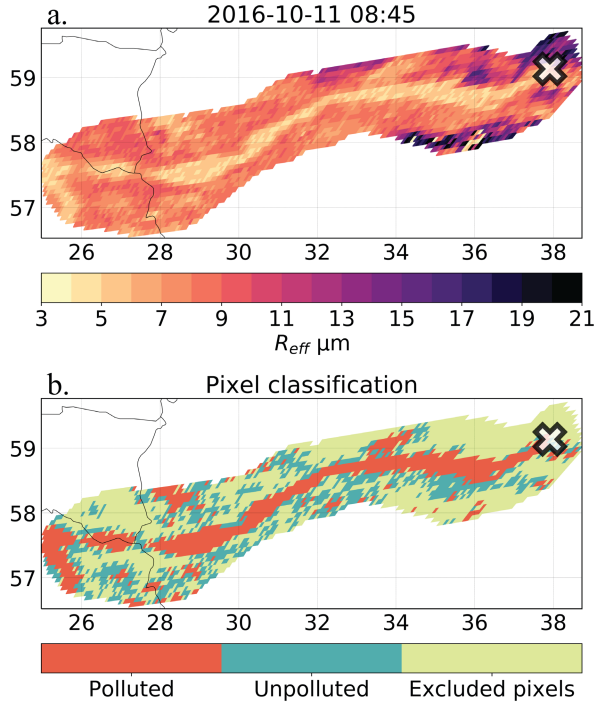

Figure 2. An example of semi-automatic cloud pixel classification to detect aerosol-polluted cloud tracks and the surrounding unpolluted clouds. (a) Manually cut region of interest; (b) Classified cloud pixels that were included in the analysis. See detailed methods in [I].

After identifying polluted and unpolluted cloud regions in SEVIRI data, I compared the cloud properties between the polluted in-track and nearby unpolluted out-of-track areas. In addition to decreases in cloud droplet size, I studied changes in the amount of cloud water (LWP). Changes in the amount of cloud water were visualised through a metric following Coakley and Walsh (2002) and Toll et al. (2019):

$$\frac{\Delta ln(COD)}{-\Delta ln(R_{eff})} = 1 - \frac{\Delta ln(LWP)}{\Delta ln(R_{eff})}. \quad \text{(Eq. 1)}$$

Parameters in Equation 1 represent the logarithmic difference between the properties of aerosol-polluted cloud tracks and the nearby surrounding unpolluted cloud regions, i.e. $\Delta ln\,(COD) = ln(COD_{polluted}) - ln(COD_{unpolluted})$. The same logic also applies to R_{eff} and LWP in Equation 1.

2.3 Analysis of the lifetime of strong anthropogenic cloud perturbations

In study [II], I estimated the lifetime of industrial aerosol-polluted cloud tracks using geostationary satellite data in a roughly similar study region as in [I]. Here, I define the lifetime as the period when the aerosol-induced cloud track was first visible until it was no longer identifiable. In study [I], I saw multiple cases where the tracks would likely extend to nighttime, but CPP limitations to daytime coverage hindered such analysis. Therefore, I relied more on the near-infrared channel data, extending the cloud observation capabilities to nighttime without losing sight of the aerosol-polluted cloud tracks. In some cases, multi-channel day and night microphysics RGBs (Lensky and Rosenfeld, 2008) provided better contrast between the polluted and unpolluted clouds. Caution should be taken with data from the periods around sunrise and sunset, owing to the poor data quality during twilight (Liang et al., 2014). For our qualitative estimations of track visibility, the twilight hours were not a critical problem. For each track case, I identified the pollution source inducing the track and the time when the track first became visible and when the track was no longer visible.

I recorded the cloud conditions when the aerosol-polluted cloud track was first identified as follows:

1) the cloud deck was present before the track appeared;
2) the track appeared right at the time of the cloud formation;
3) the cloud deck was advected over the pollution source.

Track disappearance conditions were evaluated as follows:

1) the track disappeared, but the cloud deck persisted;
2) the track disappeared because the cloud also disappeared;
3) higher level clouds moved over the track, and the track was no longer visible.

2.4 Analysis of the anthropogenic glaciation of supercooled liquid-water clouds

In [III], I studied the temporal evolution of strong anthropogenic cloud perturbations for cases where cloud fraction decreases at anthropogenic aerosol sources due to the glaciation of supercooled liquid-water clouds. I used geostationary satellite data from GOES ABI and ground-based precipitation radar data from Canada. The focus was mainly on two large industrial sites in Canada: an oil refinery on the outskirts of Regina and a copper smelter in Rouyn-Noranda. In total, 67 different industrial aerosol sources were identified in the Northern Hemisphere where glaciation events were observed. From five of those sources, 298 cloud-clearing cases were analysed in more detail. The studied aerosol

sources include heavy industrial sites like various metal processing plants (iron, steel, copper, nickel, etc.), cellulose processing factories, oil refineries, and coal-fired power plants (Table 2).

Table 2. Type of industry and specific emission sources, together with the number of cases found to induce anthropogenic aerosol-induced glaciation events in the Northern Hemisphere. This table is adapted from [III].

Field of industry	Emission sources	Number of sources
Metallurgy	Machine building, processing of steel, iron, copper, nickel, and alumina	32
Minerals	Production of cement, asphalt, and mineral fertilisers	20
Hydrocarbon combustion	Coal-fired power plants, oil refineries, and the production of petrochemicals	12
Cellulose	Production of cellulose and paper	3

It was found that anthropogenic aerosols serving as INPs explained the reduced cloud cover during the glaciation events, although emissions of heat and water vapour may also play a role. I used GOES ABI data (Rahu et al., 2024a) to study the transformation of supercooled liquid-water clouds to ice clouds and the lifetime of glaciation events. I used ground-based precipitation radar data (Rahu et al., 2024b) to study precipitation (snowfall) intensities, coverage and duration during the identified anthropogenic glaciation events. Aerosol emissions from anthropogenic sources cause plume-shaped holes in supercooled liquid water cloud decks, which have relatively similar shapes to ship-track-like CCN-polluted cloud tracks (Toll et al., 2019). Although initial cloud clearing events were identified using MODIS data from the NASA Worldview application, they were most often also detectable from GOES ABI geostationary satellite imagery to study the temporal evolution of the cloud clearings. GOES ABI spatial resolution is 2 km at the nadir and roughly 4–7 km per pixel for the two studied locations (Regina and Rouyn-Noranda), as the horizontal resolution depends on the satellite view angle.

The precipitation radar data were provided by the Meteorological Service of Canada (Rahu et al., 2024b). The analysis included data from older single-polarisation S-band and newer dual-polarisation C-band precipitation radars. The two main radar sites closest to the two aerosol sources were chosen for the study. Landrienne radar (latitude, longitude: 48.5515°, –77.8081°) is located in the Québec region, roughly 95 km from a large copper smelter in Rouyn-Noranda, Canada. Bethune radar (latitude, longitude: 50.5711°, –105.1826°) is located in the Saskatchewan province, roughly 44 km from the oil refinery in Regina. Precipitation radar allows to study the formation and coverage of precipitation areas with high spatiotemporal resolution, while satellite remote sensing lacks such capabilities. S-band and C-band radars had similar scanning characteristics.

Data included in the analysis had 0.5° resolution in azimuth and 500 meters resolution radially, with a maximum range of 240 km. Radar data were available for 77 glaciation cases for the Landrienne radar and 45 glaciation cases for the Bethune radar from 2005 to 2021. Precipitation plumes resulting from the aerosol-induced glaciation of supercooled liquid-water clouds were found in 16 and 19 cases for Bethune and Landrienne radar data, respectively. A dual-polarisation-based hydrometeor classification product was used to identify the precipitation type in the aerosol-polluted cloud regions. In all cases studied where the hydrometeor classification product was available, the precipitation plumes under investigation consisted of ice crystals. Therefore, to estimate the snowfall intensities and accumulated snowfall amount, I used the following reflectivity to snowfall (Z-S) relationship operationally used in Canada:

$$Z = 399 \cdot S^{2.21}. \quad \text{(Eq. 2)}$$

2.5 Analysis of meteorological conditions favouring aerosol-polluted cloud tracks

It is assumed that the studied heavy industrial sites emit aerosol particles more or less continuously. Yet, the aerosol-polluted cloud tracks and glaciation events occur only under specific meteorological conditions. To study the meteorological conditions favourable for the aerosol-polluted cloud tracks, ECMWF ERA5 atmospheric reanalysis (Hersbach et al., 2020) data ([I–III]; Keernik et al., 2024) and MODIS cloud top temperature datasets [III] were used. ERA5 provides gridded atmospheric variables with a high spatial resolution (31 km horizontally) and global coverage. For studies [I–II], I sampled the meteorological conditions for all the polluted cloud track locations at local noon. For study [III], the ERA5 reanalysis data were taken closest to the respective Terra overpass times to enable consistent temporal coverage with the MODIS-based cloud top temperatures. Longer-term climatological meteorological conditions were analysed for all studies to see if the days with visible pollution tracks or glaciation events stand out from the average meteorological conditions.

3. RESULTS

3.1 Diurnal evolution of cloud responses to aerosols

I studied the temporal evolution of properties of polluted cloud tracks influenced by aerosol emissions by heavy industry using CPP product (Roebeling et al., 2006; MSG-CPP, 2012) based on MSG SEVIRI satellite data. The dataset included 74 cloud tracks from 23 different days from 2006 to 2017 in the European part of Russia. I also analysed the previously sampled MODIS satellite dataset by Toll et al. (2019) with temporal coverage from morning to evening from different overpasses in different geographical locations. On average, a decrease in cloud water partially weakens the Twomey effect in both datasets (Figure 3). However, for a smaller subset of pollution track cases in SEVIRI data, there was a substantial increase in *LWP* in the afternoon, enhancing the Twomey effect substantially. In contrast, no such increase was witnessed in the early morning.

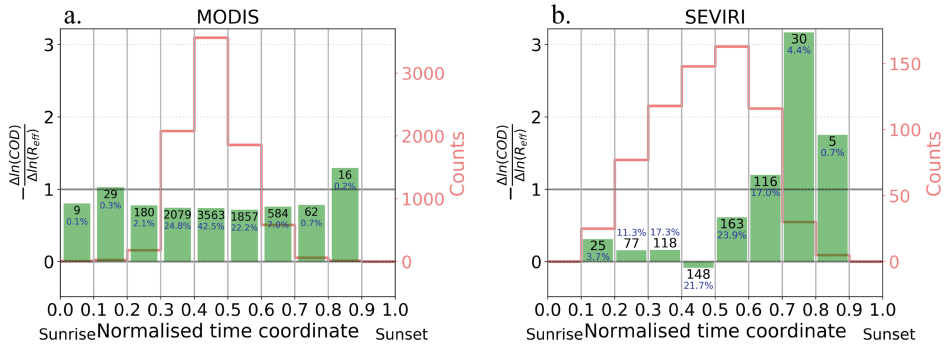

Figure 3. Diurnal changes in the ratio $-\Delta\ln(COD)/\Delta\ln(R_{eff})$ (see Methods 2.2 and [I]) averaged over all the aerosol-polluted cloud track cases included in [I]. Values above 1 show increases and values below 1 show decreases in liquid water path (*LWP*). (a) Moderate Resolution Imaging Spectroradiometer (MODIS) cases and (b) Spinning Enhanced Visible and Infrared Imager (SEVIRI) cases included in [I].

Although the spatial resolution of SEVIRI data is much lower in the study area compared to MODIS data, the polluted cloud tracks are still clearly visible from the prevailing stratocumulus cloud decks on the studied days. There is enough contrast between polluted and unpolluted areas (Figure 1), which made it possible to apply the semi-automated algorithm to distinguish polluted and unpolluted pixels from the CPP data (Figure 2).

LWP was mostly lower in the aerosol-polluted cloud tracks, but in some cases, a drastic increase in *LWP* was found in SEVIRI data around noon. On average, I saw a 26% decrease in *LWP* for polluted clouds compared to surrounding unpolluted clouds in MODIS cases, but no visible diurnal development in cloud properties could be identified. The average decrease in *LWP* for SEVIRI cases

was higher, i.e. 46%. Similarly to MODIS cases, the least square fit, considering all data, also indicated no clear trend in *LWP* response over the diurnal cycle. On the other hand, there were a few cases where cloud water increased extremely strongly in the polluted clouds in a very short time period in the afternoon (Figure 3b, [I]). The cause of the observed rapid thickening of clouds is still unclear.

Taking a broader perspective, I examined the meteorological conditions favourable for the identified aerosol-polluted cloud tracks. The aerosol-polluted cloud tracks are much more often seen in autumn months. Overall, the polluted cloud tracks appear more favourably in anticyclonic conditions with winds from the northeast (Figure 4). Also, the air mass tends to be drier above clouds with statically rather stable conditions and higher-than-average boundary layer heights (Figure 4). It is important to note that no significant diurnal cycle in meteorological conditions was identified.

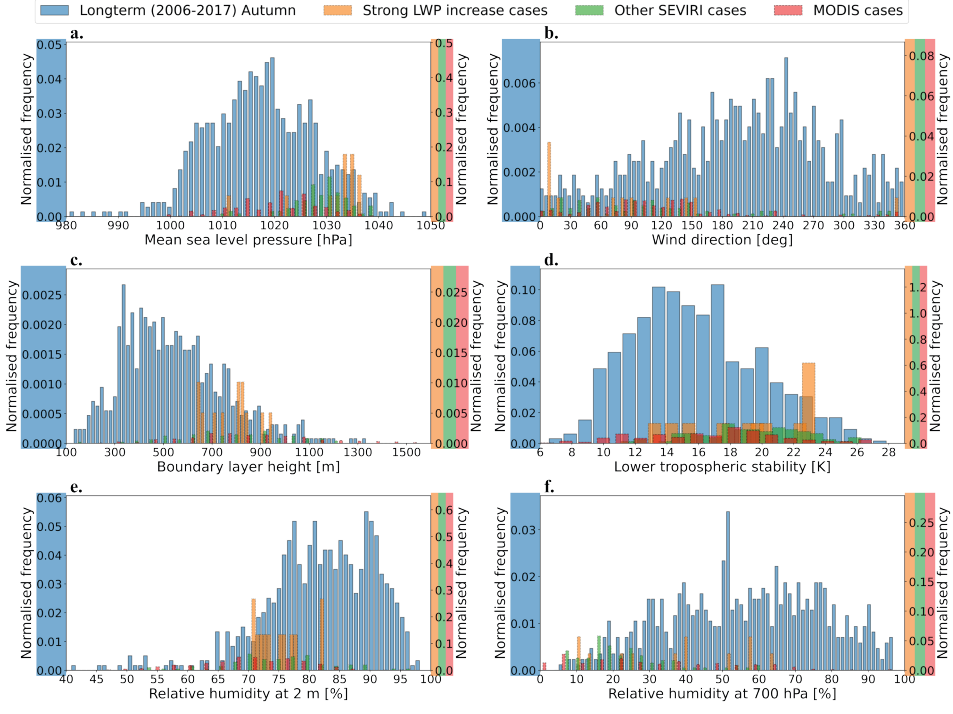

Figure 4. Frequency distributions depicting the values of various meteorological variables from European Centre for Medium-Range Weather Forecasts (ECMWF) Reanalysis v5 (ERA5) for all the Spinning Enhanced Visible and Infrared Imager (SEVIRI) cases included in [I]. (a) Mean sea level pressure [hPa], (b) Wind direction [degrees], (c) Boundary layer height [m], (d) Lower tropospheric stability [K], (e) Relative humidity at 2 m [%], (f) Relative humidity at 700 hPa level [%].

3.2 The lifetime of aerosol-polluted cloud tracks

I quantified the lifetimes of polluted cloud tracks using geostationary satellite data based on the visibility of pollution tracks in satellite images. The focus was on 19 large industrial sites in Eastern Europe, with more than a third of all cases at a single aerosol source (Cherepovets steel production site). The differences in aerosol emissions or meteorological conditions could explain the differences in track occurrence frequencies for different aerosol sources. I could often detect multiple tracks forming at various aerosol sources during the same day, although the appearance and disappearance times of the tracks could vary nevertheless.

Polluted cloud tracks can persist for several days. The average lifetime of such tracks is 18 hours, but with persisting ambient conditions favouring tracks, the tracks were visible for more than 24 hours in a quarter of the cases. In 7% of cases, the tracks' lifespan was more than 48 hours, with the most long-lived case persisting 84 hours (Figure 5). This shows that the polluted cloud tracks can live as long as favourable meteorological conditions exist. The meteorological conditions favouring the tracks are associated with anticyclonic circulation, a statically stable lower atmosphere and low relative humidity above the cloud deck, especially for long-lasting tracks. These conditions also broadly coincide with the ones favouring the occurrence of stratocumulus clouds for this region (Trofimov et al., 2022).

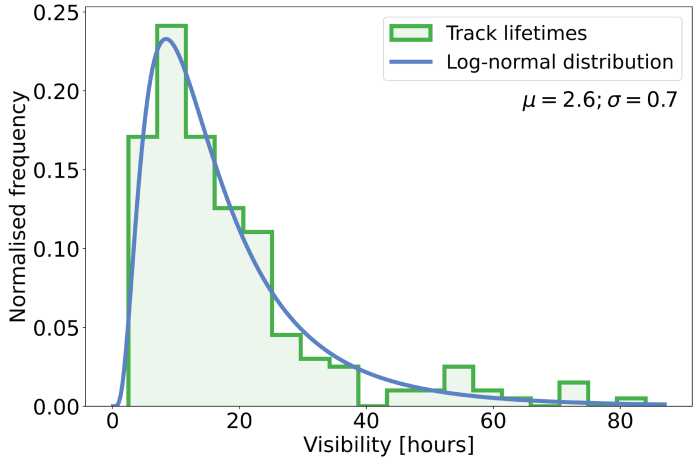

Figure 5. Aerosol-polluted industrial cloud track lifetimes (green columns) with fitted log-normal distribution (blue line, mean and standard deviation for the fitted distribution are given in the top right corner). The average lifetime of industry tracks is 18.2 hours, but it can reach multiple days [II].

Polluted cloud tracks are seen to form at all times of the day. However, there is a clear peak for the early morning (after sunrise) between 05 and 08 in UTC when the tracks form much more frequently (Figure 6) than the rest of the day. The possible explanations could be the diurnal fluctuations in the properties of the atmospheric boundary layer, or partly the selection bias for included cases due to using only the Terra satellite data for the initial selection of cases. On the other hand, the tracks were no longer visible mostly from around noon to the evening (Figure 6). This can be partially explained by complex cloud regimes for the continental study area. In 61% of the cases, the visibility of tracks was obstructed by a higher-level cloud system. This suggests that I might underestimate the real duration of the aerosol perturbations on continental clouds, as I relied on the visual identification of the tracks. Compared to the ship tracks in subtropical marine clouds, the track lifetimes are more challenging to quantify in the case of continental clouds because high clouds often overlie the studied low clouds.

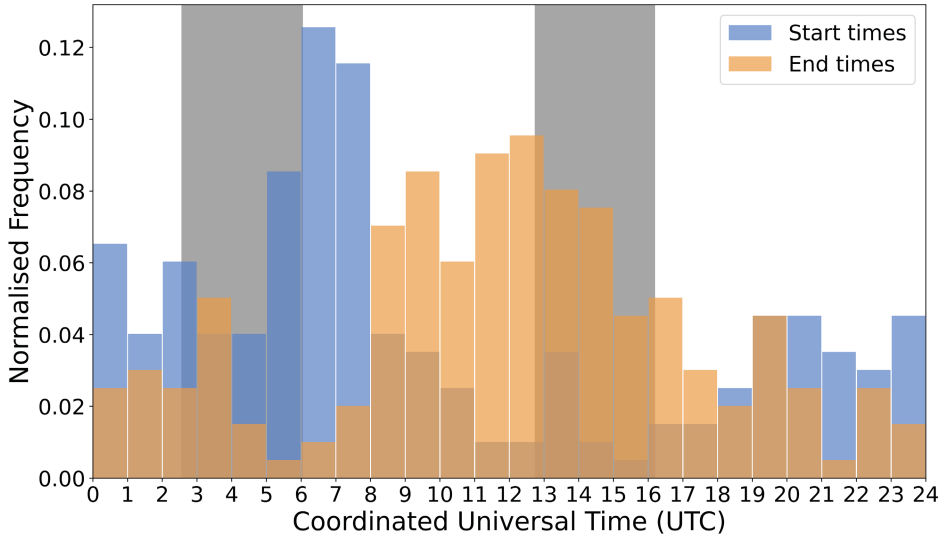

Figure 6. Aerosol-polluted industrial cloud track start times (blue columns) and end times (orange columns) [II]. Grey areas show sunrise (left) and sunset (right) times over the included track cases.

I identified the aerosol-polluted cloud tracks more often in the daytime, where the occurrence peaks before noon (between 07 to 10 UTC; Figure 7). This is fairly similar to the ship tracks on the west coast of Africa (Schreier et al., 2010). Both types of tracks occur most frequently during the daytime when the cloud brightening due to aerosol influence could lead to enhanced backscattering of solar radiation to space and a cooling effect on Earth's climate.

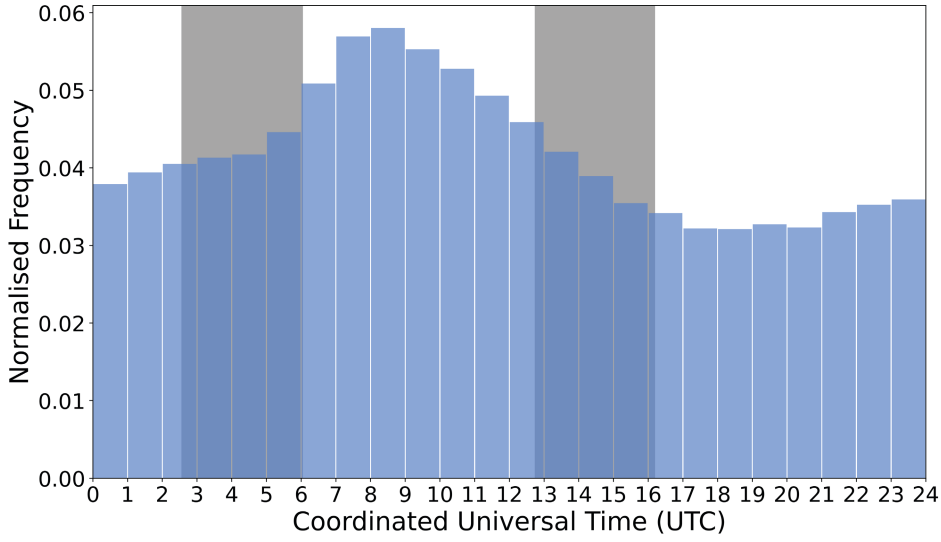

Figure 7. All the Spinning Enhanced Visible and Infrared Imager (SEVIRI) timesteps from cases included in study [II] where aerosol-polluted cloud tracks were visible. Grey areas show sunrise (left) and sunset (right) times over the included track cases.

3.3 The temporal evolution of anthropogenic glaciation of supercooled liquid-water clouds and associated snowfall events

In study [III], a phenomenon was documented where anthropogenic aerosols serving as INPs trigger glaciation events within supercooled liquid-phase clouds, converting cloud droplets into ice crystals. However, the emission of heat and water vapour may also play a role in inducing the identified glaciation events. The study identified 67 different aerosol sources in the northern hemisphere leading to glaciation events, with a detailed analysis of 298 glaciation events near five of those aerosol sources: a copper smelter in Rouyn-Noranda, Canada; an oil refinery in Regina, Canada; a metallurgical plant in Cherepovets, Russia; and cement plants in Fokino and Volsk, Russia [III].

Using satellite data from polar-orbiting Terra MODIS and geostationary GOES ABI instruments, combined with ground-based precipitation radar data (Figure 8), I observed the causal sequence of processes induced by anthropogenic INPs beginning with the formation of ice clouds within otherwise uniform supercooled liquid water cloud decks, followed by snowfall induced by ice crystal growth, and ultimately resulting in a reduction of cloud cover (Figures 9, 10, 11). In most cases, the aerosol-affected area with reduced cloud cover had a plume-like shape similar to CCN-induced ship or industrial pollution tracks. Plume-shaped CCN and INP perturbations are both narrower close to the aerosol source and grow wider further from the aerosol source (Figure 9AC). High temporal resolution GOES ABI data revealed different cloud dynamics within the polluted cloud areas, compared to the nearby unpolluted clouds. In 69% of the cases, ice clouds were identified in the aerosol-polluted area within the unpolluted liquid-phase cloud deck. I found enhanced precipitation intensities in 29% of the glaciation cases where the precipitation radar data were available (Figures 8, 9B). The hydrometeor classification product confirmed that the identified precipitation mostly consisted of ice crystals.

Based on their visibility in geostationary satellite data, the aerosol-induced glaciation events persisted for up to 17 hours with an average area of 4,066 km², while the snowfall events persisted for up to 8 hours with an average coverage of 2,161 km². Snowfall accumulations were also substantial, reaching daily totals of 15 mm with an average snowfall intensity of 1.2 mm/hour. In three instances, fresh snow on the ground with plume-shaped coverage starting right downwind of a known industrial aerosol source was seen (Figure 9D). The radar data provided very strong evidence that the events of anthropogenic glaciation of supercooled liquid-water clouds are sometimes accompanied by relatively strong and extensive snowfall, which would not have occurred without the emissions of anthropogenic INPs at strong industrial aerosol sources (Figure 10).

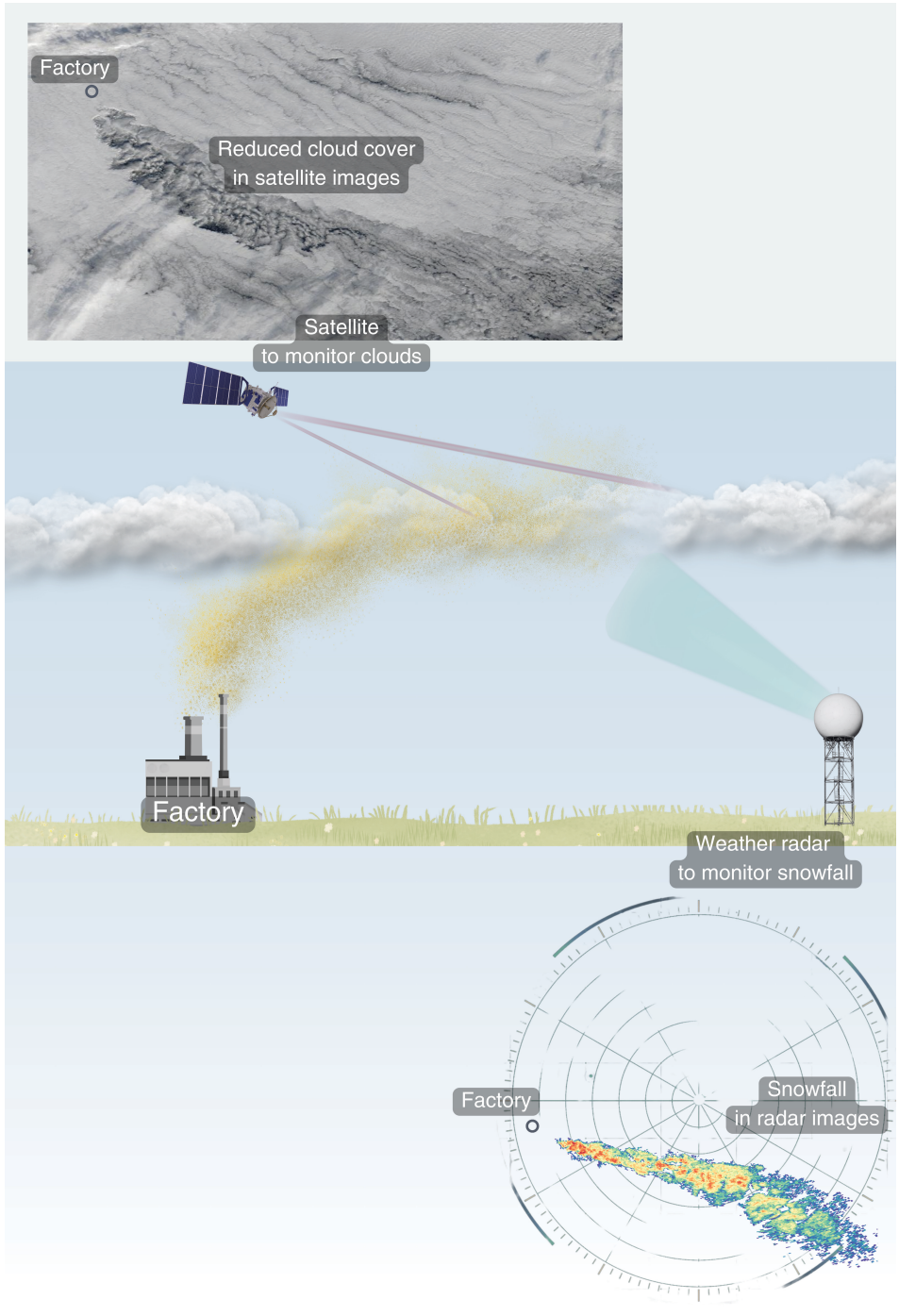

Figure 8. Monitoring the temporal evolution of anthropogenic glaciation events using both polar orbiting and geostationary satellite data and ground-based precipitation radar data enabled the development of a physical understanding of anthropogenic glaciation of supercooled liquid-water clouds [III].

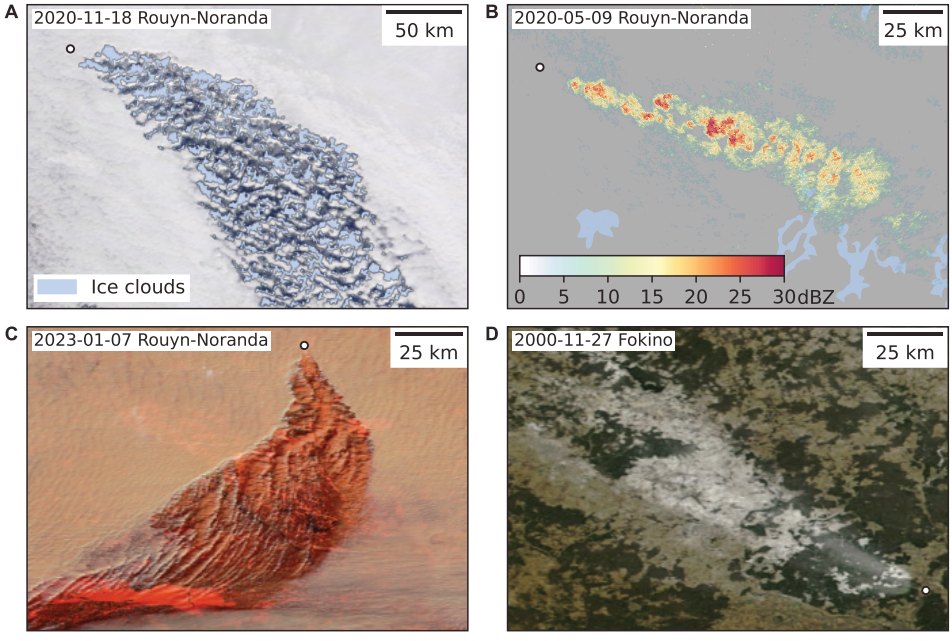

Figure 9. Anthropogenic glaciation of supercooled liquid-water clouds due to aerosols from industrial emissions acting as ice-nucleating particles (INPs), causing snowfall and reducing cloud cover [III]. (A) Ice clouds derived from Moderate Resolution Imaging Spectroradiometer (MODIS) data are surrounded by a uniform supercooled liquid phase cloud deck, downwind of Rouyn-Noranda, Canada. (B) Enhanced reflectivities from ground-based precipitation radar data showing plume-shaped snowfall downwind from a large industrial site at Rouyn-Noranda, Canada. (C) Near-infrared MODIS composite (channels 3-6-7) shows a plume-shaped area with reduced cloud cover downwind of a large industrial site at Rouyn-Noranda, Canada. (D) Plume-shaped fresh snow on the ground after a glaciation event at Fokino, Russia, seen from the MODIS true colour composite image.

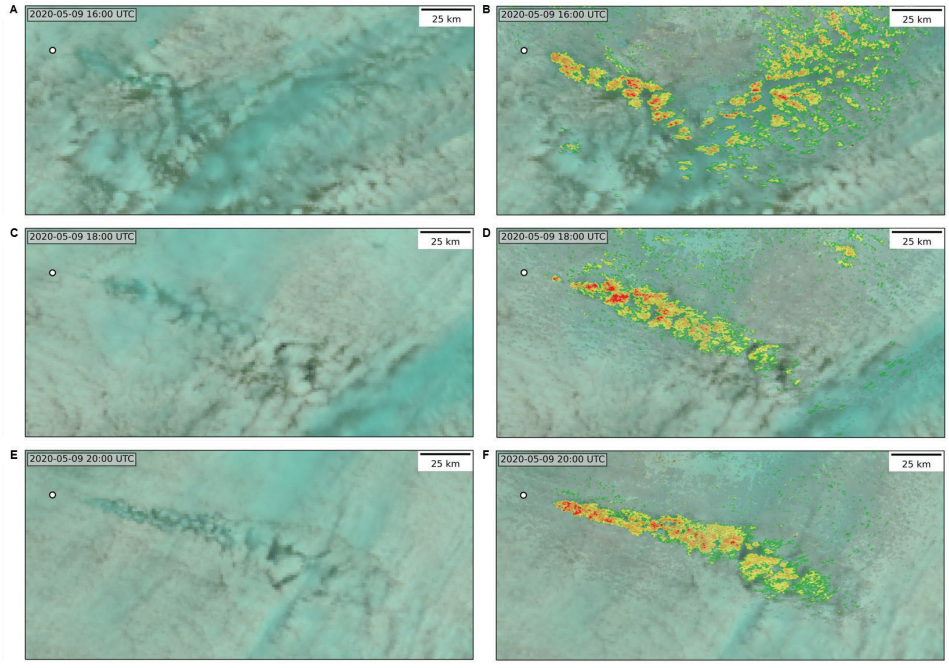

Figure 10. Geostationary Operational Environmental Satellites Advanced Baseline Imager (GOES ABI) true colour images (left column; A, C, E) for an anthropogenic glaciation event. Ground-based precipitation radar data (right column; B, D, F) overlaid on GOES ABI true colour images reveal snowfall events exactly where the glaciation takes place and cloud cover is reduced [III].

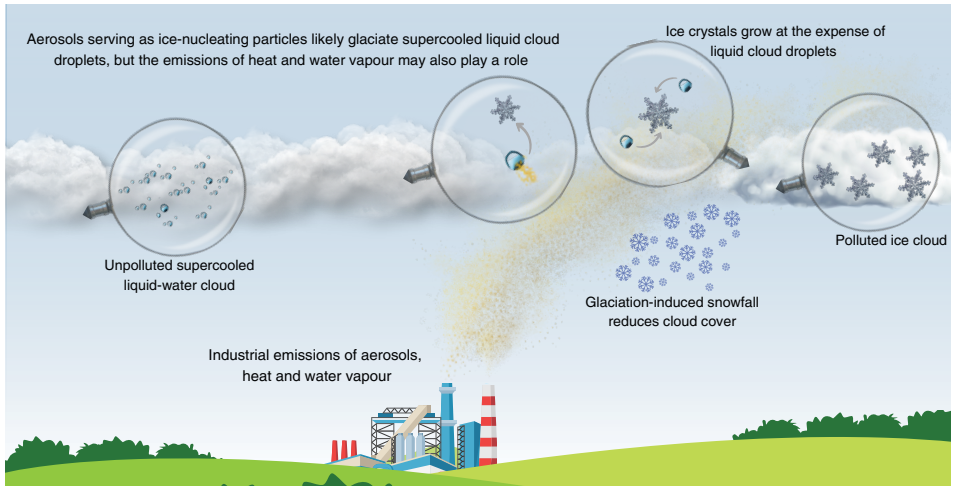

Figure 11. Developed physical understanding of the glaciation of supercooled liquid clouds due to anthropogenic aerosols [III]. After the glaciation of supercooled liquid-water clouds, the ice crystals grow through the Wegener-Bergeron-Findeisen process and produce snowfall, which can lead to decreased cloud cover.

3.4 Meteorological conditions favourable for CCN-induced and INP-induced perturbations on clouds

Specific meteorological conditions favour strong anthropogenic cloud perturbations, induced either by anthropogenic CCN or INPs. In all of the studies [I–III], study regions and times of track occurrences were different. Thus, the ambient conditions can not be compared directly. Nevertheless, there are strong similarities in the favourable conditions where these track-like cloud perturbations occur more often. ERA5 reanalysis dataset showed that both CCN- and INP-induced events are more likely to develop during high-pressure conditions with stable lower troposphere and dry air above clouds, characterised by uniform stratiform cloud decks with high cloud fraction. These conditions favour persistent stratiform clouds, allowing the aerosol perturbations to develop in the cloud decks.

Although both CCN and INP perturbations are more frequently identified in the cold season, the glaciation events occur at lower cloud-level temperatures than CCN-induced pollution tracks. MODIS cloud-top temperatures indicated that glaciation events predominantly occur at temperatures between –10 °C and –24 °C, though the specific cloud-top temperatures vary depending on the source of aerosols (Figure 12). Glaciation events occur at higher temperatures than hole punch clouds induced by airplanes, but at lower temperatures than CCN perturbations [III].

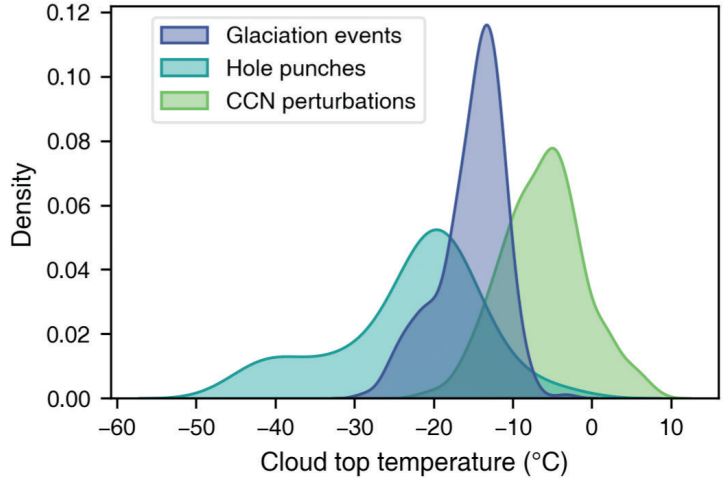

Figure 12. Cloud top temperatures from Moderate Resolution Imaging Spectroradiometer (MODIS) data show that glaciation events mostly occur at cloud top temperatures between –24 °C and –10 °C [III]. Glaciation events occur at lower temperatures than cloud condensation nuclei perturbations, but at higher subzero temperatures than aircraft-induced hole punches.

These meteorological conditions align with previous analyses of stratiform clouds susceptible to aerosol impacts, and such conditions favour the occurrence of visible cloud perturbations identifiable in satellite imagery (Trofimov et al., 2022). This does not mean that anthropogenic aerosols do not affect clouds in other meteorological situations. Such nuanced sensitivity to the surrounding meteorological conditions, leading to the strong aerosol-induced cloud perturbations, identifiable by the naked eye in the satellite images, highlights the complex relationships between aerosols and clouds, which are both strongly influenced by the meteorological conditions.

4. DISCUSSION AND CONCLUSIONS

The primary aim of the dissertation was to improve the physical understanding of how anthropogenic aerosols influence cloud properties by analysing the temporal evolution of strong aerosol perturbations using different remote sensing data sources. My study reveals novel insights into the cloud responses to industrial aerosol emissions, using high temporal resolution datasets from geostationary satellites and ground-based precipitation radars. I showed that SEVIRI data allow to study the temporal evolution of anthropogenic cloud perturbations. However, SEVIRI data are also limited in providing reliable quantitative results. Although the partial offset of the Twomey effect by the decreased *LWP* is in qualitative agreement with the analysis of MODIS data by Toll et al. (2019) and Trofimov et al. (2020), the number of aerosol-polluted cloud tracks identified in SEVIRI data should be increased in future work.

I found two different cloud water responses from the SEVIRI dataset [I]. There were track cases where polluted clouds were initially thinner in the morning, compared to the nearby unpolluted clouds, but grew substantially thicker in the afternoon. In the second group of tracks, there were no further changes in cloud properties during the day except the same thinning of clouds observed since the morning. The increase in cloud water could result from suppressed precipitation (Gunn and Phillips, 1957; Albrecht, 1989; Rosenfeld and Lensky, 1998), and the decrease in cloud water could be caused by aerosol-enhanced entrainment during the night (Ackermann et al., 2004; Bretherton et al., 2007), which could explain the decreased cloud water already from the early morning. However, the reasons for the substantial *LWP* increase in the afternoon remain unclear, as the results could also be subject to satellite retrieval biases (Grosvenor & Wood, 2014; Gryspeerdt et al., 2021; Arola et al., 2022). All the mentioned sources of uncertainties highlight the need for more detailed research considering the diurnal evolution of cloud responses to aerosols.

There are multiple additional caveats to be considered while interpreting the diurnal evolution of cloud responses to aerosols based on the SEVIRI dataset. The dataset consists only of a limited number of cases from relatively confined study regions in Eastern Europe, which is unlikely to represent the global cloud responses to aerosols. As I initially identified the aerosol-polluted cloud tracks using solely Terra MODIS data, the dataset is subject to selection bias due to possibly considering only cases with a cloud perturbation signature visible at the Terra satellite overflight time. In addition, the cloud droplet sizes in the polluted areas are at the lower limits of SEVIRI instrument theoretical retrieval capabilities of 3 μm (Finkensieper et al., 2016; Benas et al., 2017), possibly introducing retrieval errors in some areas where the effective droplet radius is very small owing to the increased aerosol loading in the cloud. As SEVIRI is a passive instrument, the resulting data quality strongly depends on the lighting conditions, i.e. the Sun's position relative to the satellite's field of view. The data are associated with larger uncertainties with non-optimal retrieval conditions at higher

solar zenith angles in the early morning and late evening (Grosvenor & Wood, 2014). This resulted in a quality drop for early morning and late evening data. Qualitatively, the best results were probably obtained around local noon when the study area was better illuminated.

Another important issue with SEVIRI data is the lower spatial resolution compared to polar orbit satellite instruments like MODIS. As the width of industry tracks is often tens of kilometres, they still stand out in the SEVIRI data. Nevertheless, identifying narrower tracks is more challenging. Caution must also be taken when using the cloud mask within the CPP dataset (Finkensieper et al., 2016; Benas et al., 2017). Cloud mask specifies if an observed pixel is cloudy or not, with an additional category for cloud-contaminated pixels. I used the cloud mask pixel classification to exclude low-quality pixels from the data, but the classification for heavily polluted cloud regions also changed over time. The properties of polluted clouds could change so much that the cloud mask algorithm altered the pixel classification from cloudy pixels to cloud-contaminated pixels, even if the cloud amount did not change. Further research using data from the recently launched FCI instrument onboard the MTG satellite (Ouaknine et al., 2017; Martin and Abdon, 2019) could help to provide more reliable insights into the temporal evolution of cloud responses to anthropogenic aerosols in industry tracks.

I found that continental aerosol-polluted cloud tracks can persist as long as favourable meteorological conditions and suitable clouds persist [II]. Based on the visibility, the average lifetime of the aerosol-polluted cloud tracks is 18 hours, but I saw multiple cases with lifetimes exceeding 48 hours. The aerosol-polluted cloud tracks form and persist in a statically stable lower troposphere with drier, anticyclonic conditions. Although the distribution of lifetimes resembles the subtropical ship tracks on the west coast of Africa (Schreier et al., 2010), the complex continental cloud regime significantly impacts the lifetimes of the cloud tracks. Due to a relatively coarse spatial resolution of SEVIRI data (about 10 km in the study region), many smaller tracks were excluded from the study due to difficulties detecting them from geostationary satellite data. Considering the limitations of the methods, I likely underestimated the actual lifetimes of the continental aerosol-polluted cloud tracks.

The long lifetime of aerosol-polluted cloud tracks indicates they can be used to infer the causal relationships between aerosols and clouds. With persisting optimal ambient meteorological conditions and the presence of clouds favourable for the pollution track formation, the track lifetime can easily exceed the timescale associated with cloud adjustments to aerosol-induced cloud droplet number perturbations (Glassmeier et al., 2021). Sampling the temporal evolution of cloud responses to aerosols along the longest-lived aerosol-polluted cloud tracks could help to quantify the aerosol-induced changes in cloud properties better. Moreover, analysing the along-track temporal evolution of aerosol impacts on clouds using geostationary satellite data could result in more reliable observational constraints for aerosol climate forcing.

Study [III] highlighted that anthropogenic aerosols can glaciate supercooled liquid cloud droplets, although the emissions of heat and water vapour may also play a role. The glaciation effect was visible in multiple remote sensing datasets with different retrieval capabilities. While MODIS data offered crucial high-resolution spatial information for identifying anthropogenic glaciation events, MODIS data lack the temporal resolution for detailed analysis of fast-evolving cloud processes. As the cloud perturbations cover up to thousands of square kilometres, the geostationary GOES ABI data allowed us to track the temporal evolution of anthropogenic glaciation events with a temporal resolution of 5 minutes.

Geostationary satellite data showed that clouds within the aerosol-polluted regions had different properties compared to the nearby unpolluted clouds. Moreover, I frequently saw a different cloud regime emerging in the aerosol-polluted areas, compared to the nearby unpolluted clouds. As the occurrence and the intensity of precipitation are relatively challenging to retrieve from satellite instruments, ground-based precipitation radars provided unprecedented insight into the glaciation-induced snowfall due to the Wegener-Bergeron-Findeisen process following the formation of first ice crystals (Storelvmo and Tan, 2014; Wegener, 1911; Bergeron, 1935; Findeisen, 1938). Combining ground-based precipitation radar and geostationary satellite data revealed that the snowfall occurs exactly in the same plume-shaped aerosol-polluted regions where the cloud fraction is lower due to the glaciation. This multi-instrument approach enabled us to establish a clearer process-level understanding of the mechanism of anthropogenic glaciation events, providing evidence of the impacts of anthropogenic INPs on clouds. If the impact of anthropogenic INPs is not limited to the immediate surroundings of strong industrial aerosol hot spots, anthropogenic INPs could influence Earth's climate. However, further research is needed to better understand which anthropogenic aerosols serve as INPs and whether anthropogenic INPs exert a climate forcing.

FUNDING AND DATA AVAILABILITY

This work was funded by the Estonian Research Council grants PSG202 and PRG1726. I acknowledge the use of MODIS satellite imagery from the NASA Worldview application (https://worldview.earthdata.nasa.gov), part of the NASA ESDIS. SEVIRI satellite data are available through EUMETSAT DAC, and MSG CPP product can be accessed through KNMI Data Platform (MSG-CPP, 2012). GOES ABI data were downloaded via Goes2go Python package (https://blaylockbk.github.io/goes2go/_build/html/index.html). Study [I] specific time-steps and cut-out regions are available at https://datadoi.ee/handle/33/341 (Rahu and Toll, 2021). The software used to process SEVIRI data for study [I] can be found at https://github.com/jorahu/pollution_tracks_from_SEVIRI_data. Aerosol-polluted cloud track lifetime data used in study [II] is available at https://datadoi.ee/handle/33/509 (Rahu and Toll, 2023). GOES ABI satellite data were processed with the Satpy Python package (https://satpy.readthedocs.io/en/stable/). Sunrise/sunset-related data processing was done using the Astral package (https://astral.readthedocs.io/en/latest/). GOES ABI specific data (i.e. timesteps) included in study [III] along with animated videos of the cases can be found at https://datadoi.ee/handle/33/652 (Rahu et al., 2024a). Canadian precipitation radar data used in study [III] are available at https://datadoi.ee/handle/33/653 (Rahu et al., 2024b). Wradlib (https://docs.wradlib.org/en/latest/) Python package was used to process precipitation radar data. More related datasets for study [III] with Python codes can be found at https://datadoi.ee/handle/33/610 (Toll et al., 2024). Single-level ERA5 data for meteorological background information was downloaded from CDS from https://doi.org/10.24381/cds.adbb2d47, and data from different pressure levels from https://doi.org/10.24381/cds.bd0915c6.

SUMMARY IN ESTONIAN

Tugevate inimtekkeliste pilvehäirituste ajalise arengu uurimine aitab paremini mõista aerosoolide mõju pilvedele

Tööstusrevolutsioonijärgne kliimasoojenemine on justkui köievedu inimtekkeliste kasvuhoonegaaside soojendava mõju ja aerosoolide jahutava mõju vahel. Aerosooliosakesed on mikroskoopilised tahked ja vedelad atmosfääri pihustunud õhusaasteosakesed, mis muudavad atmosfääri vähem läbipaistvaks. Aerosooliosakesed mõjutavad oluliselt aga ka pilvede omadusi, kuna käituvad pilvetekketuumadena vedelas faasis pilvepiiskade tekkimisel ja jäätekke tuumadena jääpilvede tekkimisel. Aerosooliosakeste mõju pilvedele on suurima määramatusega inimtegevuse kliimamõju komponent, kusjuures taoline suhteliselt suur määramatus takistab senisest usaldusväärsemate kliimaprojektsioonide loomist. Pilvede omaduste ja aerosooliosakeste vahel on tugev meteoroloogiline kovariatsioon. Meteoroloogiline kovariatsioon tähendab, et meteoroloogilised tingimused määravad suuresti ära nii pilvede kui ka aerosoolide omadused. Seetõttu on inimtekkeliste aerosooliosakeste põhjuslikku mõju pilvedele ülimalt keeruline kindlaks teha.

Aerosooliosakeste mõju pilvedele saab edukalt uurida, kasutades loomulikke eksperimente meteoroloogilisest kovariatsioonist põhjustatud müra ületamiseks. Loomulikud eksperimendid on sellised olukorrad, kus eksperimendilaadsed tingimused tekivad teadlaste otsese sekkumiseta. Aerosool-pilved interaktsioonide puhul on loomulikeks eksperimentideks olukorrad, kus inimtekkeliste aerosoolide poolt mõjutatud pilved on selgelt lähiümbruses asuvatest saastumata pilvedest eristatavad ning aerosoolse saaste allikas on teada. Selliste loomulike eksperimentide alla liigituvad näiteks laevade või suurte tööstuste emissioonide tõttu tekkinud pilvehäiritused. Nendel pilvehäiritustel, nn laevade- või tööstuse saastejälgedel, on ümbritsevatest pilvedest selgelt eristuvad omadused. Taolistes saastejälgedes eeldame, et inimtekkelise aerosoolse saaste hulk on ainuke erinev tegur saastunud ja saastumata ala võrdlemisel, sest meteoroloogilised tingimused on ruumilise läheduse tõttu samad. Seetõttu saamegi hinnata, milline on lisandunud aerosoolide mõju pilvede omadustele. Tööstusjälgi on varasemalt uurinud polaarorbiidi satelliitinstrumendi MODIS (*Moderate Resolution Imaging Spectroradiometer*) andmetest Toll jt (2019, https://doi.org/10.1038/s41586-019-1423-9), Trofimov jt (2020, https://doi.org/10.1029/2020JD032575) ning Trofimov jt (2022, https://doi.org/10.1029/2021jd035871). Käesoleva töö uudsus seisneb selles, et uurisin saastejälgede ajalist arengut geostatsionaarsete satelliitide ja maapealsete sademeradarite andmete põhjal.

Töö üldine eesmärk oli parandada füüsikalist arusaama inimtekkeliste aerosooliosakeste mõjust pilvedele, analüüsides saasteosakeste poolt mõjutatud pilvedes toimuvaid muutusi. Minu töö täpsemateks eesmärkideks oli:

1. Tuvastada aerosoolse saaste poolt mõjutatud pilved geostatsionaarsete satelliitinstrumentide andmetest [I–III].
2. Välja selgitada, kuidas aerosoolide mõju pilvedele päeva jooksul muutub [I].

3. Teha kindlaks aerosoolse saaste poolt mõjutatud pilvede eluiga vastavalt nende tuvastatavusele geostatsionaarsetest satelliitandmetest [II].
4. Luua füüsikaline arusaam alla 0 °C jahtunud veepilvede lumestumise nähtusest, mis toimub inimtekkelise aerosoolse õhusaaste mõjul [III].
5. Teha kindlaks inimtekkelise veepilvede lumestumise tagajärjel tekkinud lumesadude intensiivsus ja kestus, kasutades selleks maapealsete sademeradarite andmeid [III].

Töö eesmärkidele ja põhitulemustele vastavad teesid on järgnevad:

1. Tööstuslikud saastejäljed pilvedes on geostatsionaarsete satelliitide andmetest usaldusväärselt tuvastatavad, võimaldades uurida kiireid ajalisi muutusi saastunud pilvede omadustes [I–III].
2. Teatud meteoroloogiliste tingimuste korral muutuvad saastunud pilved (võrreldes ümbritsevate saastumata pilvedega) päeva jooksul paksemaks [I].
3. Tööstussaaste mõju pilvedele on pikaealine, ulatudes paljudel juhtudel päevadeni [II].
4. Tööstusjäljed on tugevalt mõjutatud kohalikust pilverežiimist ja ümbritsevatest meteoroloogilistest tingimustest [II].
5. Inimtekkelised õhusaasteosakesed mitmetest erinevatest tööstusallikatest, näiteks metallide ja mineraalide töötlemisest, käituvad jäätekke tuumadena [III].
6. Geostatsionaarsete satelliitandmete ja maapealsete sademeradarite andmete kombineerimisel tuvastati põhjuslik järgnevus alla 0 °C jahtunud veepiiskade jäätumisest, kuni lumesadude tekke ja sellele järgnenud vähenenud pilvisuseni [III].

Töös kasutasin andmeid kahelt geostatsionaarselt satelliitidilt. Peamine andmeallikas oli MSG SEVIRI (*Meteosat Second Generation Spinning Enhanced Visible and Infrared Imager*) andmestik ning sellest loodud pilve füüsikaliste omaduste produkt CPP (*Cloud Physical Properties*). SEVIRI instrumendi mõõteala katab nii Aafrika kui ka Euroopa, võimaldades 15-minutilise ajasammuga uurida pilvede omadusi. CPP produkt kasutab nähtava valguse kanalite mõõtmisi ning on seetõttu kasutatav ainult päevasel ajal, kui saab registreerida aluspinnalt ja pilvedelt tagasipeegeldunud päikesekiirgust. CPP produkti abil saime kvantitatiivselt uurida muutusi pilvede omadustes. Saastejälgede eluea hindamiseks öisel ajal oli võimalik kasutada lähisinfrapuna kanali mõõtmisi. Teine töös kasutatud geostatsionaarse satelliidi instrument oli GOES ABI (*Geostationary Operational Environmental Satellites Advanced Baseline Imager*), mille peamine mõõteala on Põhja-Ameerika. Selle andmeid kasutades uurisime alla 0 °C jahtunud veepilvede lumestumist kahe suure tööstusallika läheduses Kanadas. Siin olid kasutusel veel ka Kanada Meteoroloogiateenistuse kahe maapealse sademeradari andmed, millest oli võimalik hinnata atmosfääris esinevate sademete ruumilist jaotust, intensiivsust ja kaudselt ka sademete liiki. Viimase kahe andmestiku omavaheline kombineerimine oli antud uuringus võtmetähtsusega inimtekkelise aerosoolse saaste tõttu aset leidnud pilvede lumestumisest füüsikalise arusaama loomisel.

Artiklis [I] leidsin, et inimtekkeliste aerosoolide poolt põhjustatud saastejäljed on ruumiliselt piisavalt ulatuslikud, et hoolimata geostatsionaarsete satelliitide instrumentide kehvema ruumilise lahutusega andmetest neid usaldusväärselt ümbritsevatest saastumata pilvedest eristada. Saastunud pilvealade eristamine võimaldas uurida saastunud pilvede veehulka, pilvede optilist paksust, pilvepiiskade efektiivset raadiust ja nende omaduste muutusi ajas. Aegridade analüüs näitas, et tööstussaaste poolt mõjutatud pilved muutuvad päeva jooksul keskmiselt paksemaks, võrreldes ümbritsevate saastumata pilvedega. Kuna uuritavad saasteallikad asusid satelliitinstrumendi mõõteala äärealadel, siis oli suureks väljakutseks andmete kvaliteet. Seetõttu on tulemuste usaldusväärsus ja globaalne esinduslikkus piiratud.

Artiklis [II] leidsin, et tööstuslike aerosoolide häiritused on pilvedes pikaealised ja võivad kesta ka mitu järjestikust päeva. See, kui kaua mingi saastejälg satelliidiandmetest tuvastatav oli, sõltus tugevalt meteoroloogilistest tingimustest: seni kuni sobivad tingimused jälgede tekkeks püsisid, püsis enamasti ka saaste mõju pilvedele. Saastejälgede pikaealisus näitab, et aerosoolide poolt põhjustatud pilvede häiritusi peaks saama edukalt kasutada, uurimaks aerosoolide mõju pilvedele ja kliimale, kui valida sobivad juhtumid ja alad, kus suurenenud aerosooliosakeste kontsentratsioonile vastav häiritus pilvede omadustes on tasakaalustunud.

Artiklis [III] avastasime inimtekkelise pilvede lumestumise nähtuse, kus inimtekkelised aerosooliosakesed põhjustavad alla 0 °C jahtunud vedelas faasis pilvepiiskade jäätumise. Samas võivad siin rolli mängida ka soojuse ja veeauru emissioonid. Jääkristallid hakkavad ümbritsevate vedelas faasis pilvepiiskade arvelt kasvama (Wegener-Bergeron-Findeiseini protsess), kuna küllastav veeaururõhk on samal temperatuuril jää kohal madalam kui vee kohal. Kui jääkristallid on piisavalt suureks kasvanud, sajavad nad lumena alla, põhjustades pilvkatte vähenemise. Just geostatsionaarse satelliidi andmete kombinatsioon maapealsete sademeradari andmetega tagas olulised tõendid lumestumise nähtuses olulist rolli mängivate protsesside põhjusliku ajalise järjestuse kinnituseks. Alla 0 °C jahtunud veepilvede inimtekkelise lumestumise avastamine on oluline täiendus füüsikalisele arusaamale, mis kirjeldab aerosoolide mõju pilvedele. Aga küsimus, kas inimtekkeline veepilvede lumestumise nähtus omab ka laiemat mõju Maa kliimale, vajab edasist uurimist.

Näitasin, et inimtekkeliste aerosoolide poolt põhjustatud pilvede häirituste ajalise arengu uurimine geostatsionaarsete satelliitandmete ja maapealsete sademeradari andmete abil võimaldas edukalt luua parema füüsikalise arusaama aerosoolide mõjust pilvedele. Kui varasemalt on tugevaid aerosoolide poolt põhjustatud pilvehäiritusi uuritud peamiselt polaarorbiidi satelliitandmete põhjal, siis minu töö näitab, et ka edaspidi oleks oluline kasutada ajalist arengut jälgida võimaldavaid geostatsionaarsete satelliitide mõõtmisandmeid. Kuigi mitmed töös uuritud füüsikalised protsessid vajavad veel edasisi põhjalikumaid uuringuid, võib minu töö tulemusest tõusta kasu kliimamudelite arendamisel ja senisest usaldusväärsemate kliimaprojektsioonide loomisel.

REFERENCES

Ackerman, A. S., Kirkpatrick, M. P., Stevens, D. E., & Toon, O. B. (2004). The impact of humidity above stratiform clouds on indirect aerosol climate forcing. *Nature*, *432*(7020), 1014–1017. https://doi.org/10.1038/nature03174

Albrecht, B. A. (1989). Aerosols, cloud microphysics, and fractional cloudiness. *Science*, *245*(4923), 1227–1230. https://doi.org/10.1126/science.245.4923.1227

Aminou, D. M. A. (2002). MSG's SEVIRI instrument. *ESA Bulletin(0376–4265)*, (111), 15–17.

Arola, A., Lipponen, A., Kolmonen, P., Virtanen, T. H., Bellouin, N., Grosvenor, D. P., Gryspeerdt, E., Quaas, J. & Kokkola, H. (2022). Aerosol effects on clouds are concealed by natural cloud heterogeneity and satellite retrieval errors. *Nature Communications*, *13*(1), 7357. https://doi.org/10.1029/2019RG000660

Bellouin, N., Quaas, J., Gryspeerdt, E., Kinne, S., Stier, P., Watson-Parris, D., et al. (2020). Bounding global aerosol radiative forcing of climate change. *Reviews of Geophysics*, *58*(1), e2019RG000660. https://doi.org/10.1029/2019rg000660

Benas, N., Finkensieper, S., Stengel, M., van Zadelhoff, G. J., Hanschmann, T., Hollmann, R., & Meirink, J. F. (2017). The MSG-SEVIRI-based cloud property data record CLAAS-2. *Earth System Science Data*, *9*(2), 415–434. https://doi.org/10.5194/essd-9-415-2017

Benas, N., Solodovnik, I., Stengel, M., Hüser, I., Karlsson, K.-G., Håkansson, N., Johansson, E., Eliasson, S., Schröder, M., Hollmann, R., & Meirink, J. F. (2023). CLAAS-3: the third edition of the CM SAF cloud data record based on SEVIRI observations, *Earth Syst. Sci. Data*, *15*, 5153–5170, https://doi.org/10.5194/essd-15-5153-2023

Bergeron, T. (1935). On the physics of cloud and precipitation. *L'Association de Météorologie de L'U.G.G.I.* Vol. 2, p. 156

Bretherton, C. S., Blossey, P. N., & Uchida, J. (2007). Cloud droplet sedimentation, entrainment efficiency, and subtropical stratocumulus albedo. *Geophysical Research Letters*, *34*(1), L03813. https://doi.org/10.1029/2006GL027648

Chen, J., Wu, Z. J., Gong, X., Qiu, Y., Chen, S., Zeng, L., & Hu, M. (2024). Anthropogenic dust as a significant source of ice-nucleating particles in the urban environment. *Earth's Future*, 12. https://doi.org/10.1029/2023EF003738

Christensen, M., Gettelman, A., Cermak, J., Dagan, G., Diamond, M., Douglas, A., ... & Yuan, T. (2022). Opportunistic experiments to constrain aerosol effective radiative forcing. *Atmospheric Chemistry and Physics Discussions*, *2021*, 1–60. https://doi.org/10.5194/acp-22-641-2022

Coakley, J. R., Bernstein, R. L., & Durkee, P. A. (1987). Effect of Ship-Stack Effluents on Cloud Reflectivity. *Science*, *237*(4818), 1020–1022. https://doi.org/10.1126/science.237.4818.1020

Coakley Jr, J. A., & Walsh, C. D. (2002). Limits to the aerosol indirect radiative effect derived from observations of ship tracks. *Journal of the Atmospheric Sciences*, *59*(3), 668–680. https://doi.org/10.1175/1520-0469(2002)059<0668:LTTAIR>2.0.CO;2

Cziczo, D. J., Stetzer, O., Worringen, A., Ebert, M., Weinbruch, S., Kamphus, M., ... & Lohmann, U. (2009). Inadvertent climate modification due to anthropogenic lead. *Nature geoscience*, *2*(5), 333–336. https://doi.org/10.1038/ngeo499

Findeisen, W. (1938). Die kolloidmeteorologischen Vorgänge bei der Niederschlagsbildung. *Meteorologische Zeitschrift*, *55*, 121–133

Finkensieper, S., Meirink, J.F., van Zadelhoff, G.-J., Hanschmann, T., Benas, N., Stengel, M., Fuchs, P., Hollmann, R., Werscheck, M. (2016). CLAAS-2: CM SAF CLoud property dAtAset using SEVIRI – Edition 2, *Satellite Application Facility on Climate Monitoring*. https://doi.org/10.5676/EUM_SAF_CM/CLAAS/V002

Glassmeier, F., Hoffmann, F., Johnson, J. S., Yamaguchi, T., Carslaw, K. S., & Feingold, G. (2021). Aerosol-cloud-climate cooling overestimated by ship-track data. *Science*, *371*(6528), 485–489. https://doi.org/10.1126/science.abd3980

Goren, T., Chourdhury, G., Kretzschmar, J., & McCoy, I. (2024). Co-variability drives the inverted-V sensitivity between liquid water path and droplet concentrations. *EGUsphere*, *2024*, 1–18. https://doi.org/10.5194/egusphere-2024-2245

Grosvenor, D. P., & Wood, R. (2014). The effect of solar zenith angle on MODIS cloud optical and microphysical retrievals within marine liquid water clouds. *Atmospheric Chemistry and Physics*, *14*, 7291–7321. https://doi.org/10.5194/acp-14-7291-2014

Gryspeerdt, E., Quaas, J., & Bellouin, N. (2016). Constraining the aerosol influence on cloud fraction. *Journal of Geophysical Research: Atmospheres*, *121*(7), 3566–3583. https://doi.org/10.1002/2015JD023744

Gryspeerdt, E., Goren, T., & Smith, T. W. P. (2021). Observing the timescales of aerosol-cloud interactions in snapshot satellite images. *Atmospheric Chemistry and Physics*, *21*(8), 6093–6109. https://doi.org/10.5194/acp-21-6093-2021

Gunn, R., & Phillips, B. B. (1957). An experimental investigation of the effect of air pollution on the initiation of rain. *Journal of Atmospheric Sciences*, *14*(3), 272–280. https://doi.org/10.1175/1520-0469(1957)014<0272:AEIOTE>2.0.CO;2

Hersbach, H., Bell, B., Berrisford, P., Hirahara, S., Horányi, A., Muñoz-Sabater, J., ... & Thépaut, J. N. (2020). The ERA5 global reanalysis. *Quarterly Journal of the Royal Meteorological Society*, *146*(730), 1999–2049. https://doi.org/10.1002/qj.3803

IPCC, 2023: Climate Change 2023: Synthesis Report. Contribution of Working Groups I, II and III to the Sixth Assessment Report of the Intergovernmental Panel on Climate Change [Core Writing Team, H. Lee and J. Romero (eds.)]. IPCC, Geneva, Switzerland, pp. 35–115. https://doi.org/10.59327/IPCC/AR6-9789291691647

Keernik, H., Rahu, J., & Toll, V. (2024). Meteorological conditions characteristic of anthropogenic glaciation of supercooled liquid-water clouds and of anthropogenic CCN perturbations on clouds. https://datadoi.ee/handle/33/649

Lensky, I. M., & Rosenfeld, D. (2008). Clouds-aerosols-precipitation satellite analysis tool (CAPSAT). *Atmospheric Chemistry and Physics*, *8*(22), 6739–6753. https://doi.org/10.5194/acp-8-6739-2008

Liang, C. K., Mills, S., Hauss, B. I., & Miller, S. D. (2014). Improved VIIRS Day/Night Band Imagery With Near-Constant Contrast, *IEEE Transactions on Geoscience and Remote Sensing*, *52*(11), 6964–6971. https://doi.org/10.1109/TGRS.2014.2306132

Manshausen, P., Watson-Parris, D., Christensen, M.W., Jalkanen, J.-P., & Stier, P. (2022). Invisible ship tracks show large cloud sensitivity to aerosol. *Nature*, 610, 101–106. https://doi.org/10.1038/s41586-022-05122-0

Martin, P., & Abdon, S. (2019). FCI Instrument on-Board Meteosat Third Generation Satellite-Critical Design Review Outcome and Development Status. In *2019 Joint Satellite Conference*. AMS. https://doi.org/10.1117/12.2599152

Mauger, G. S., & Norris, J. R. (2007). Meteorological bias in satellite estimates of aerosol-cloud relationships. *Geophysical Research Letters*, *34*(16). https://doi.org/10.1029/2007GL029952

MSG-CPP (2012). Royal Netherlands Meteorological Institute (KNMI), https://msgcpp.knmi.nl/

Ouaknine, J., Viard, T., Napierala, B., Foerster, U., Fray, S., Hallibert, P., ... & Carel, J. L. (2017). The FCI on board MTG: Optical design and performances. In *International Conference on Space Optics—ICSO 2014* (Vol. 10563, pp. 617–625). SPIE. https://doi.org/10.1117/12.2304144

Platnick, S., Ackerman, S., King, M., et al. (2015). MODIS Atmosphere L2 Cloud Product (06_L2). NASA MODIS Adaptive Processing System, Goddard Space Flight Center, USA. http://dx.doi.org/10.5067/MODIS/MOD06_L2.061

Quaas, J., Arola, A., Cairns, B., Christensen, M., Deneke, H., Ekman, A. M. L., Feingold, G., Fridlind, A., Gryspeerdt, E., Hasekamp, O., Li, Z., Lipponen, A., Ma, P.-L., Mülmenstädt, J., Nenes, A., Penner, J. E., Rosenfeld, D., Schrödner, R., Sinclair, K., Sourdeval, O., Stier, P., Tesche, M., van Diedenhoven, B., & Wendisch, M. (2020). Constraining the Twomey effect from satellite observations: issues and perspectives. *Atmospheric Chemistry and Physics*, *20*(23), 15079–15099. https://doi.org/10.5194/acp-20-15079-2020

Rahu, J., & Toll, V. (2021). Anthropogenic aerosol impacts on clouds from SEVIRI satellite data. https://datadoi.ee/handle/33/341

Rahu, J., & Toll, V. (2023). Lifetime of anthropogenic aerosol perturbations on clouds seen from geostationary SEVIRI satellite data. https://datadoi.ee/handle/33/509

Rahu, J., Post, P., & Toll, V. (2024a). GOES ABI satellite data to study anthropogenic glaciation of supercooled liquid-water clouds downwind of industrial air pollution hot spots. https://datadoi.ee/handle/33/652

Rahu, J., Voormansik, T., Michelson, D., Hung, E., Donaldson, N., & Toll, V. (2024b). Ground-based precipitation radar data to study glaciation of supercooled liquid-water clouds downwind of anthropogenic air pollution hot spots. https://datadoi.ee/handle/33/653

Roebeling, R. A., Feijt, A. J., & Stammes, P. (2006). Cloud property retrievals for climate monitoring: Implications of differences between Spinning Enhanced Visible and Infrared Imager (SEVIRI) on METEOSAT-8 and Advanced Very High Resolution Radiometer (AVHRR) on NOAA-17. *Journal of Geophysical Research*, *111*(D20), D20210. https://doi.org/10.1029/2005JD006990

Rosenfeld, D., & Lensky, I. M. (1998). Satellite-Based Insights into Precipitation Formation Processes in Continental and Maritime Convective Clouds. *Bulletin of the American Meteorological Society*, *79*(11), 2457–2476. https://doi.org/10.1175/1520-0477(1998)079<2457:SBIIPF>2.0.CO;2

Salomonson, V. V., Barnes, W. L., Maymon, P. W., Montgomery, H. E., & Ostrow, H. (1989). MODIS: advanced facility instrument for studies of the Earth as a system, *IEEE Transactions on Geoscience and Remote Sensing*, *27*(2), 145–153. https://doi.org/10.1109/36.20292

Schreier, M., Joxe, L., Eyring, V., Bovensmann, H., & Burrows, J. P. (2010). Ship track characteristics derived from geostationary satellite observations on the west coast of southern Africa. *Atmospheric Research*, *95*(1), 32–39. https://doi.org/10.1016/j.atmosres.2009.08.005

Schmit, T. J., Griffith, P., Gunshor, M. M., Daniels, J. M., Goodman, S. J., & Lebair, W. J. (2017). A Closer Look at the ABI on the GOES-R Series. *Bulletin of the American Meteorological Society*, *98*(4), 681–698. https://doi.org/10.1175/BAMS-D-15-00230.1

Schmit, T. J., & Gunshor, M. M. (2020). Chapter 4 – ABI Imagery from the GOES-R Series, *Elsevier*, 23–34. https://doi.org/10.1016/B978-0-12-814327-8.00004-4

Small, J. D., Chuang, P. Y., Feingold, G., & Jiang, H. (2009). Can aerosol decrease cloud lifetime?. *Geophysical Research Letters*, *36*(16). https://doi.org/10.1029/2009GL038888

Storelvmo, T., & Tan, I. (2015). The Wegener-Bergeron-Findeisen process–Its discovery and vital importance for weather and climate. *Meteorologische Zeitschrift*, *24*(4), 455–461. http://dx.doi.org/10.1127/metz/2015/0626

Suzuki, K., Stephens, G. L., & Lebsock, M. D. (2013). Aerosol effect on the warm rain formation process: Satellite observations and modeling. *Journal of Geophysical Research: Atmospheres*, *118*(1), 170–184. https://doi.org/10.1002/jgrd.50043

Toll. V., Keernik, H., Rahu, J., Trofimov, H., Post, P., Manshausen, P., Christensen, M., Michelson, D., Donaldson, N., Hung, E. (2024). Anthropogenic glaciation of supercooled liquid water clouds. https://datadoi.ee/handle/33/610

Toll, V., Christensen, M., Quaas, J., & Bellouin, N. (2019). Weak average liquid-cloud-water response to anthropogenic aerosols. *Nature*, *572*(7767), 51–55. https://doi.org/10.1038/s41586-019-1423-9

Trofimov, H., Bellouin, N., & Toll, V. (2020). Large-scale industrial cloud perturbations confirm bidirectional cloud water responses to anthropogenic aerosols. *Journal of Geophysical Research: Atmospheres*, *125*(14), e2020JD032575. https://doi.org/10.1029/2020JD032575

Trofimov, H., Post, P., Gryspeerdt, E., & Toll, V. (2022). Meteorological conditions favorable for strong anthropogenic aerosol impacts on clouds. *Journal of Geophysical Research: Atmospheres*, *127*(4), e2021JD035871. https://doi.org/10.1029/2021jd035871

Twomey, S. (1974). Pollution and the planetary albedo. *Atmospheric Environment*, *8*(12), 1251–1256. https://doi.org/10.1016/0004-6981(74)90004-3

Watson-Parris, D., & Smith, C. J. (2022). Large uncertainty in future warming due to aerosol forcing. *Nature Climate Change*, *12*(12), 1111–1113. https://doi.org/10.1038/s41558-022-01516-0

Wegener, A. (1911). Thermodynamik der Atmosphäre. Barth, Leipzig. https://doi.org/10.1007/978-3-642-90779-1_3

Yuan, T., Song, H., Wood, R., Oreopoulos, L., Platnick, S., Wang, C., ... & Wilcox, E. (2023). Observational evidence of strong forcing from aerosol effect on low cloud coverage. *Science Advances*, *9*(45), eadh7716. https://doi.org/10.1126/sciadv.adh7716

Zhao, B., Wang, Y., Gu, Y., Liou, K.-N., Jiang, J., H., Fan, J., Liu, X., Huang, L., & Yung, Y. L. (2019). Ice nucleation by aerosols from anthropogenic pollution. *Nat. Geosci*. 12, 602–607. https://doi.org/10.1038/s41561-019-0389-4

ACKNOWLEDGEMENTS

I would like to express my deepest gratitude to my supervisors Assoc. Prof. Velle Toll and Prof. Piia Post, who never stopped supporting and guiding me, even when I myself did not see much value in continuing this work. Without them, this thesis would have never been born. They always found time to help me with any issue or topic, be it scientific or personal, to help and discuss. I appreciate the patience they had with me and the effort they put into my development as a person and a researcher.

Special thanks go to all the colleagues at the Centre for Climate Research who provided loads of mental support and great discussions over the lunch table, especially Heido Trofimov, Kristel Uiboupin and Hannes Keernik. Undoubtedly, a strong role model and pillar of support was Tanel Voormansik, who went through the same process at the same time and always understood the difficulties I suffered and encouraged me to keep going throughout my studies. Special thanks go to our Canadian colleagues who provided the much-needed radar data for one of the papers.

Sincere regards go to my colleagues at the Estonian Environment Agency, who allowed me to keep my job while studying and provided all the leaves that I needed for the most difficult parts of the studies.

I also thank my closest family members and my wife, Ida Rahu, for their endless support. Without this stability, the whole thing would not have been possible. Deepest love goes to our dog Lumi, who provided cuddles whenever needed and forced me to take breaks and get some fresh air to clear my mind and soul.

It is impossible to write down every name whom I encountered during this period who more or less contributed with either direct scientific advice, helped with coding or general discussions about nature, radars, dogs, technology or tacos. Everyone who recognises themselves regarding any of the topics, you know who you are, I bow to you and thank you.

PUBLICATIONS

CURRICULUM VITAE

Name: Jorma Rahu
Date of birth: 27.03.1992
Citizenship: Estonian
Gender: Male
Email: Jorma.Rahu@ut.ee

Education

2019–2025	University of Tartu, PhD in Physics
2016–2018	University of Tartu, MSc in Physics
2011–2015	University of Tartu, BSc in Physics

Languages

Estonian, English

Professional employment

2023–…	University of Tartu, Institute of Physics; Specialist in Climate Physics
2018–…	Estonian Environment Agency; Chief Specialist in Radar Meteorology
2022–2023	University of Tartu, Institute of Physics; Junior Research Fellow in Physics
2019–2022	University of Tartu, Institute of Physics; Specialist

Research interests

Atmospheric and climate sciences: anthropogenic climate forcing; aerosol-cloud interactions; remote sensing; radar meteorology

Publications

Toll, V., **Rahu, J.**, Keernik, H., Trofimov, H., Voormansik, T., Manshausen, P., ... & Bellouin, N. (2024). Glaciation of liquid clouds, snowfall, and reduced cloud cover at industrial aerosol hot spots. Science, 386(6723), 756–762.

Rahu, J., Voormansik, T., Michelson, D., Hung, E., Donaldson, N., Keernik, H., Trofimov, H., Post, P., Toll, V. (2024). Ground-based Precipitation Radar Signatures of Anthropogenic Snowfall Events Downwind of Industrial Air Pollution Hot Spots. In the 12th European Conference on RADar in Meteorology and Hydrology (ERAD 2024).

Toll, V., & **Rahu, J.** (2023). Strong anthropogenic cloud perturbations can persist for multiple days. Journal of Geophysical Research: Atmospheres, 128(9), e2022JD038146.

Rahu, J., & Toll, V. (2023). Novel insights into aerosol-cloud interactions enabled by analysing the temporal evolution of strong anthropogenic cloud perturbations. In EGU General Assembly Conference Abstracts (pp. EGU-7090).

Rahu, J., Trofimov, H., Post, P., & Toll, V. (2022). Diurnal evolution of cloud water responses to aerosols. Journal of Geophysical Research: Atmospheres, 127(10), e2021JD035091.

Rahu, J., Post, P., Toll, V. (2021). Diurnal Evolution of Anthropogenic Aerosol Impacts on Clouds. In American Meteorological Society: Virtual AMS 101st Annual Meeting.

Honours and Awards

2024 University of Tartu Research Achievement of the Year: "Discovering glaciation of supercooled clouds at anthropogenic air pollution hot spots" (Research team member)

2024 Best Oral Presentation Award for "Ground-based Precipitation Radar Signatures of Anthropogenic Snowfall Events Downwind of Industrial Air Pollution Hot Spots" presented at The 12th European Conference on RADar in Meteorology and Hydrology (ERAD 2024), September 9–13

2021 Second Place/Student Poster Presentation Award for poster named "Diurnal Evolution of Anthropogenic Aerosol Impacts on Clouds" presented at the 101st American Meteorological Society Annual Meeting, January 10–15

ELULOOKIRJELDUS

Nimi: Jorma Rahu
Sünniaeg: 27.03.1992
Kodakondsus: eestlane
Sugu: mees
E-mail: Jorma.Rahu@ut.ee

Haridus

2019–2025	Tartu Ülikool, füüsika õppekava, PhD
2016–2018	Tartu Ülikool, füüsika õppekava, MSc
2011–2015	Tartu Ülikool, füüsika õppekava, BSc

Keelteoskus

Eesti, inglise

Töökogemus

2023–…	Tartu Ülikool, Füüsika Instituut; kliimafüüsika spetsialist
2018–…	Keskkonnaagentuur; radarmeteoroloogia peaspetsialist
2022–2023	Tartu Ülikool, Füüsika Instituut; füüsika nooremteadur
2019–2022	Tartu Ülikool, Füüsika Instituut; spetsialist

Teadustöö põhisuunad

Atmosfääri- ja kliimafüüsika: inimtegevuse kliimamõju; aerosoolide ja pilvede vastasmõju; kaugseire, radarmeteoroloogia

Publikatsioonid

Toll, V., **Rahu, J.**, Keernik, H., Trofimov, H., Voormansik, T., Manshausen, P., ... & Bellouin, N. (2024). Glaciation of liquid clouds, snowfall, and reduced cloud cover at industrial aerosol hot spots. Science, 386(6723), 756–762.

Rahu, J., Voormansik, T., Michelson, D., Hung, E., Donaldson, N., Keernik, H., Trofimov, H., Post, P., Toll, V. (2024). Ground-based Precipitation Radar Signatures of Anthropogenic Snowfall Events Downwind of Industrial Air Pollution Hot Spots. In the 12th European Conference on RADar in Meteorology and Hydrology (ERAD 2024).

Toll, V., & **Rahu, J.** (2023). Strong anthropogenic cloud perturbations can persist for multiple days. Journal of Geophysical Research: Atmospheres, 128(9), e2022JD038146.

Rahu, J., & Toll, V. (2023). Novel insights into aerosol-cloud interactions enabled by analysing the temporal evolution of strong anthropogenic cloud perturbations. In EGU General Assembly Conference Abstracts (pp. EGU-7090).

Rahu, J., Trofimov, H., Post, P., & Toll, V. (2022). Diurnal evolution of cloud water responses to aerosols. Journal of Geophysical Research: Atmospheres, 127(10), e2021JD035091.

Rahu, J., Post, P., Toll, V. (2021). Diurnal Evolution of Anthropogenic Aerosol Impacts on Clouds. In American Meteorological Society: Virtual AMS 101st Annual Meeting.

Tunnustused ja auhinnad

2024 Tartu Ülikooli aasta teadustegu „Inimtekkelise õhusaaste põhjustatud pilvede lumestumise avastamine“ (Uurimisrühma liikmena)

2024 Parima suulise ettekande auhind konverentsil ERAD 2024 ettekandega „Ground-based Precipitation Radar Signatures of Anthropogenic Snowfall Events Downwind of Industrial Air Pollution Hot Spots“

2021 II koht posterettekandega üliõpilaste kategoorias 101. AMS konverentsil ettekandega „Diurnal Evolution of Anthropogenic Aerosol Impacts on Clouds“

DISSERTATIONES GEOPHYSICALES UNIVERSITATIS TARTUENSIS

1. **Andres Kuusk.** The hot-spot effect in plant canopy reflectance. Tartu, 1991.
2. **Tiit Nilson.** Radiative transfer in non-homogeneous plant canopies. Tartu, 1991.
3. **Helgi Arst.** Atmosfääri ja mere kiirguskarakteristikud looduskeskkonna seisundi informaatoritena (vene keeles). Tartu, 1991.
4. **Juha Sarkkula.** Measuring and modelling water currents and quality as a part of decision making process for water pollution control. Tartu, 1992.
5. **Piia Post.** On the two radiatively effective cloud parameters. Tartu, 1993.
6. **Aadu Mirme.** Electric aerosol spectrometry. Tartu, 1994.
7. **Aare Luts.** Mathematical simulation of the evolutions of air ions. Tartu, 1995.
8. **Tiit Kutser.** Estimation of water quality in turbid inland and coastal waters by passive optical remote sensing. Tartu, 1997.
9. **Ülle Kikas.** Atmospheric aerosol in the Baltic region. Tartu, 1998.
10. **Tarmo Kõuts.** Processes of deep water renewal in the Baltic sea. Tartu, 1999.
11. **Anu Reinart.** Underwater light field characteristics in different types of Estonian and Finnish lakes. Tartu, 2000.
12. **Marko Kaasik.** Parameterisation of atmospheric boundary layer in the numerical model of air pollution transport. Tartu, 2000.
13. **Janek Laanearu.** Topographically constrained deep-water flows in channels. Tartu, 2001.
14. **Urmas Raudsepp.** Wind-driven circulation in the gulf of Riga. Tartu, 2001.
15. **Urmas Hõrrak.** Air ion mobility spectrum at a rural area. Tartu, 2001.
16. **Marko Vana.** Formation and evolution of atmospheric aerosol size spectrum by the occurrence of nucleation burst events in the atmospheric boundary layer; transport of the climatically active particulate air pollution. Tartu, 2002.
17. **Veljo Kimmel.** Analysis of methods of air quality assessment. Applications in Estonia. Tartu, 2002.
18. **Oleg Okulov.** Variability of atmospheric transparency and precipitable water in Estonia. Tartu, 2003.
19. **Aarne Männik.** Implementation and validation of the nonhydrostatic adiabatic core of the numerical weather prediction model hirlam. Tartu, 2003.
20. **Matti Mõttus.** Shortwave solar radiation field inside willow canopy. Tartu, 2004.
21. **Kalev Rannat.** Long weakly nonlinear waves in geophysical applications. Tartu, 2007.
22. **Rigel Kivi**. Observations of ozone, polar stratospheric cloud and water vapour profiles in the arctic. Tartu, 2007.

23. **Erko Jakobson.** Spatial and temporal variability of atmospheric column humidity. Tartu, 2009, 125 p.
24. **Sander Mirme.** Development of nanometer aerosol measurement technology. Tartu, 2011, 118 p.
25. **Hannes Keernik.** Estimating methods and variability of atmospheric humidity over the Baltic Region and the Arctic. Tartu, 2015, 105 p.
26. **Martin Kannel.** Development of Broadband Aerosol Optical Depth Models. Tartu, 2016, 168 p.
27. **Krista Alikas**. From research to applications: monitoring optically complex waters with MERIS/ENVISAT data. Tartu, 2016, 172 p.
28. **Velle Toll.** Direct radiative impacts of atmospheric aerosols on meteorological conditions over Europe. Tartu, 2016, 148 p.
29. **Margit Aun.** Dependence of UV radiation on climate factors. Reconstruction of UV doses in Estonia for past years. Tartu, 2017, 124 p.
30. **Siiri Suursoo.** Natural Radioactivity in Cambrian-Vendian Groundwater – Analytical Procedures, Monitoring of Drinking Water Treatment Technology, and Associated Changes in Groundwater Quality. Tartu, 2019, 146 p.
    Heido Trofimov. Polluted clouds at air pollution hot spots help to better understand anthropogenic impacts on Earth's climate. Tartu, 2022, 96 p. Published in *Dissertationes Physicae Universitatis Tartuensis*, *128*.
31. **Tanel Voormansik.** Long-term datasets of dual-polarisation weather radar help detect and nowcast convective storms including extreme precipitation, lightning, and hail. Tartu, 2023, 124 p.